Office of Naval Research

Contract N5ori-76 · Task Order No. 1 · NR-078-011

ELECTROMAGNETIC SCATTERING FROM TWO PARALLEL CONDUCTING CIRCULAR CYLINDERS

By

R. V. Row

May 1, 1953

Technical Report No. 170

Cruft Laboratory
Harvard University
Cambridge, Massachusetts

Office of Naval Research

Contract N5ori-76

Task Order No. 1

NR-078-011

Technical Report

on

Electromagnetic Scattering from Two Parallel Conducting Circular Cylinders

by

R. V. Row

May 1, 1953

The research reported in this document was made possible through support extended Cruft Laboratory, Harvard University, jointly by the Navy Department (Office of Naval Research), the Signal Corps of the U. S. Army, and the U. S. Air Force, under ONR Contract N5ori-76, T. O. 1.

Technical Report No. 170

Cruft Laboratory

Harvard University

Cambridge, Massachusetts

TR170

Electromagnetic Scattering from Two Parallel Conducting Circular Cylinders

by

R. V. Row

Abstract

The problem of scattering of an incident cylindrical (or plane) electromagnetic wave by an arbitrary array of perfectly conducting parallel circular cylinders is solved for the case of the electric vector parallel to the axes of the cylinders. The use of a Green's theorem and application of the appropriate boundary conditions results in a set of integral equations for the unknown surface currents on each cylinder. These currents may be expanded in a complex Fourier series and the set of integral equations thus transformed into an infinite set of linear algebraic equations in the unknown Fourier coefficients. For a plane wave incident on a planar grating the connection with Wessel's work is shown.

To simplify the computations the theory is specialized to the case of two identical cylinders. The solution of a finite number of the linear equations is considered by exact and approximate numerical methods. In addition, neglect of the coupling between different current modes yields a simple formula for the scattered field in which the effect of coupling is quite apparent.

For the two cylinders equidistant and far from the source the scattered field is computed from these approximations for cylinders as large as a wavelength in diameter and spacings ranging from one to four wavelengths between centers. The validity of the various approximations is determined by comparison with microwave measurements carried out at a wavelength of 3.185 cm in a parallel plate region. The theory indicates significant departures from the predictions of the independent scattering hypothesis and these have been confirmed experimentally.

TR170

Electromagnetic Scattering from Two Parallel Conducting Circular Cylinders

by

R. V. Row

Cruft Laboratory, Harvard University

Cambridge, Massachusetts

1. Introduction

The problem of multiple scattering of freely propagating waves has interested numerous investigators for the past sixty years. Various theoretical analyses of particular problems have been based upon a solution of the scalar wave equation subject to appropriate boundary conditions. The complexity of these problems calls for simplifying assumptions either in their initial formulation or in dealing with the final results. These assumptions are invariably based upon consideration of scatters which are either 1) very small compared to a wavelength, and may be closely spaced, or 2) spaced so that their separation is much larger than their dimensions and a wavelength, so that each scatter scatters independently. Actually no results have been obtained previously for the case where the dimensions of and spacings between scatters are comparable to a wavelength. It is for this latter case that coupling between scattering elements should be large, and interesting departures from the results of the independent scattering hypothesis are expected.

This report considers a combined theoretical and experimental study of the scalar problem of scattering of an incident cylindrical electromagnetic wave by two infinitely long parallel, identical, and perfectly conducting cylinders (for spacings and diameters comparable to a wavelength) arranged with the incident electric field parallel to their axes.

This section presents an historical introduction to the scalar multiple scattering problem. The two succeeding sections introduce the specific problem above in more general terms by considering the scattering by an arbitrary array of any number of such perfectly conducting cylinders of arbitrary diameters. By specialization to the case of scattering of a plane incident wave by a planar grating of indentical cylinders the connection with another grating theory is shown.

The complexity of the theory for the infinite grating and line source, which would be necessary to take account of experimental conditions, is so great as to preclude any calculations being based on this theory, except for the case of very large spacing between cylinders. For this reason the theory is further specialized in Section 4 to the case of a line source and two identical cylinders. Some of the consequences of this theory are considered and methods of obtaining numerical results to check with field measurements are discussed.

Although the problem of diffraction by a grating of wires has received considerable attention in the literature dating back to the turn of the century,[1,2,3] there remain certain aspects which have not been satisfactorily investigated, namely, the effects of the size of the cylinders on mutual effects and the use of a line source of excitation in place of the usual plane wave. Consideration of coupling effects between scatters is of fundamental physical interest, whereas the use of a line source of excitation is an attempt to bring the theoretical assumptions into closer approximation with feasible experimental arrangements. At best, as was seen in Technical Report No. 153, one may obtain experimentally various approximations to the elusive and unnatural plane wave. However, if the object of diffraction measurement is to correlate the experimental data with a theoretical model assuming plane-wave excitation, then one is restricted to the study of relatively small centers of scattering, and for simplicity it is best to use a line source.*

A recent set of measurements by Groves[4] on the transmission properties of parallel wire grids using a point source indicated considerable disagreement with the theoretical results of Wessel[5] based on plane-wave incidence. This disagreement is attributed by Groves to the use of a point source and clearly indicates that the existing theory does not give accurate correlation with experiment.

A perusal of the literature on scattering from several obstacles reveals that theoretical work on problems of this type has been limited chiefly to cases where the field quantities involved are essentially scalar in nature. Such an approach to the problems of multiple scattering while not valid for the most general cases of electromagnetic scattering nevertheless sheds a good deal of light on the essentially unique properties of these problems which may be attributed to mutual coupling.

Of all possible configurations of multiple scatters that of the infinite diffraction grating made up of a planar array of parallel identical circular cylinders or strips has received the greatest attention. The reasons for this concentration of effort are fairly obvious and are briefly stated here. Firstly, the vector wave equation for the electromagnetic field may be separated into two independent scalar wave equations which may then be solved separately. Secondly, with plane-wave excitation the total field exhibits a periodic nature so that the resulting theoretical expression for the field may be conveniently expressed in simple form enabling the effects of mutual coupling and size of scatterer to

\- - - - - - -

*The problem of diffraction of a spherical wave by a cylinder has been solved by F. Oberhettinger (see Annalen der Physik (5) 43, 136-160 (1943)) and the corresponding problem with a conducting wedge replacing the cylinder by H. Carslaw (loc. cit.) Proc. London Math. Soc. 17: 30, 121 (1899). However, in both cases the expressions for the resulting field reduce to relatively simple form only in the far zone.

be more readily understood than with a finite grating or any other type of excitation.

Recent papers by Twersky,[6] Shmoys[7] and Groves[4] give a fairly complete set of references to the literature on this and related problems. These sources have been useful to the writer in evaluating the advantages and drawbacks of the various theories on the grating of parallel wires and in deciding how to formulate a theory which takes into account both coupling and a line source of primary excitation. It is therefore timely to give at this juncture a critical evaluation of the work done on this problem to date.

The simplest assumption that can be made in any multiple scattering problem is that all the obstacles scatter independently This idea goes back at least as far as Rayleigh,[8] who first employed it in his theory of the scattering of light by small particles in the sky,* although a possible earlier source of this idea is to be found in Thomas Young's[9] theory of optical diffraction. The usual theory for the optical diffraction grating is based on this simplification and the results of such an analysis predict accurately the angular position of the various spectral orders. However, Wood[10] observed the phenomenon of almost discontinuous changes in the intensity of some lower-order spectra as a speculum metal grating was rotated so as to change the angle of incidence. To explain this effect Rayleigh[3] found it necessary to take account of mutual interaction effects between elements of the grating. His recognition of this fact started a tide of investigation in the diffraction grating which is still active. Apart from J. J.

- - - - - - -

*In measuring the diffraction from two parallel identical conducting cylinders, R. D. Kodis (see Cruft Lab. Progress Report Nos. 18 and 19, Harvard University (1951)) found that even for cylinders a wavelength in diameter the independent scattering hypothesis gives reasonable predictions of the trend of near zone field measurements for cylinders spaced as closely as 6 wavelengths between centers.

Thompson's[1] attempt* to solve the problem of reflection and transmission of an electromagnetic wave by a grating of closely spaced wires Lamb[2] gave the first clear theoretical solution valid for small wires and close spacing by referring to the analogous static potential problem. His results received experimental confirmation at the hands of Shaefer and Laugwitz[11] who employed decimeter electromagnetic waves from a Hertzian(spark) oscillator.

Ignatowsky[12] was the first to develop a general theory of scattering from an infinite grating of identical elements using a formal solution of Maxwell's field equations satisfying the appropriate boundary conditions. He expressed the total field as a superposition of the incident field and an integral over the surface of each element in the grating (without specifying any particular shape of grating element). Because of the periodic nature of the boundary conditions he expands the total field in a series of plane waves analogous to the propagating and evanescent modes in a waveguide. (The waveguide point of view in treating diffraction gratings has been developed quite recently in a number of papers by Marcuvitz,[13] Miles,[14] and Shmoys.[7])** The formal process of satisfying the boundary conditions leads to a set of equations for the mode coefficients which may be expressed in a neat form involving a number of single integrals over the surface of a grating element. Due, however, to the cumbersome notation used, and Ignatowsky's failure to apply the results of his analysis to any specific grating

*It is interesting to note that Thompson expands the field in a Fourier series of the same period as the grating spacing, an idea developed apparently independently by Ignatowsky twenty years later. However, Thompson's use of the electromagnetic boundary conditions in determining the Fourier coefficients is not clear and his results were discarded in favor of Lamb's by the experimenters Shaefer and Laugwitz.

**Shmoys' recently published paper (see ref. 27) gives a variational method for calculating the mode coefficients in an analysis essentially the same as Ignatowsky's.

problems, his very general results have been ignored by later workers in favor of a simpler approach to their particular problems.

Shaefer and Reiche[15] seem to be the first to have expanded the scattered field from an array (of circular cylinders) in a series of Hankel functions, although the idea of expanding the field scattered from a single cylinder in such a series had been used earlier by Seitz.[16]

They neglect mutual coupling (i.e., they assume grating spacing much greater than a wavelength) and solve for the coefficients in the series by applying the electromagnetic boundary conditions. Their chief interest in the analysis is to determine the effect of the material of the grating elements on the diffraction effects. To first order, at least, they show that the location of the far-zone minima is independent of the grating material. Their analysis of the diffraction grating is more realistic than previous analyses in that they consider the effect of a finite number of elements in the grating and find, as might be expected, that the scattered field is subject to significant amplitude changes from that expected for the case of the infinite grating. Their paper contains no numerical computations to show these effects graphically or otherwise.

Concurrently with Ignatowsky, Zaviska[17] developed an analysis of diffraction from an arbitrary array of parallel cylinders by expanding the scattered field in a series of Hankel functions representing cylindrical waves radiating from each cylinder. By using various expansion theorems for Bessel functions he matched the fields to the boundary conditions at the surface of each cylinder. This procedure resulted in an infinite number of linear algebraic equations in an infinite number of unknowns which in principle could be solved for the coefficient of each cylincrical wave in the original expansion of the scattered field. He suggests a method of iteration for solving these equations and gives an approximate method for determining the effect of the wire radius on the field; in essence this is a criterion for specifying what is meant when one speaks of "small" wires. Zaviska applied this interesting theory to an array of two very thin wires to explain the experimental results of scattering measurements from a thin dielectric cylinder made by Shaefer and Grossmann.[18] However, he did not apply his method to the study of scattering by wires of cross-sectional dimensions and spacing comparable to wavelength where one may expect interesting departures from the simple independent-scattering hypothesis.

Recently Wessel[5] developed an analysis of scattering from an array of parallel filamentary conductors based on deriving the scattered field from a vector potential derivable from the currents in the wires of the grating. He gives simple expressions for the transmission coefficient of the grating based on plane-wave incidence, his results being valid for small wires and closely spaced grating elements. Wessel's theory has received excellent experimental confirmation at the hands of Esau, Ahrens and Kebbel.[19]

Franz[20] has rederived Wessel's results by solving the wave equation directly in plane polar coordinates without the intermediate step of the vector potential. He also considered the problem of two parallel gratings, and showed an interesting resonance in the transmission coefficient as the spacing between the gratings is changed. As with Wessel, his results are limited to the infinite grating of small wires and plane-wave incidence.

Within the last few years Miles[14] and Shmoys[7] have considered the grating problem using a variational method. In essence they Fourier-analyze the total field to reduce the complexity of the mathematical problem to a stage which requires only the solution of a single integral equation, resulting from the requirements imposed by the electromagnetic boundary conditions. This procedure leaves a series of plane-wave mode-coefficients as the unknowns to be determined, and at this point in the analysis they introduce the well-known variational method of Levine and Schwinger to express the quantities of physical interest in a form which permits a simpler computational problem than that resulting in Ignatowsky's paper. However, the authors do not consider how they will determine the necessary current distributions on their scattering elements for use as trial functions in the variational formulas. Miles paper gives results which yield the transmission coefficient of the grating as a unit for plane-wave incidence, while Shmoys' results, in principle at least, allow the scattered field to be computed everywhere, although as with Ignatowsky's earlier analysis, this requires the summing of a series of modes; the rate of convergence depending on the degree of coupling between grating elements. Marcuvitz is referred to in Shmoys'[7] and Groves'[4] papers as having considered grating problems from an integral equation point of view and also as having applied variational techniques to the computation of their far-zone transmission properties. Unfortunately, his work does not appear in any of the regular journals or in any readily accessible place in the literature.

Twersky[6] considers the problem of diffraction by arbitrary array of parallel cylinders and accounts for coupling by a system of "multiply scattered" waves. In this novel analysis the first-order wave is that resulting from the scattering of the incident field by each cylinder acting independently, the second order takes into account the rescattering of these first-order waves by each scatterer, and so on to higher order scattered waves. This formulation is chiefly useful when the scatterers are relatively loosely coupled so that only the first few orders need be computed. In a recent paper, Twersky[21] applies this method of analysis to the problem of the diffraction grating of small wires and explains the "anomalies" noticed by Wood.[8] For the case of the infinite array of small cylinders and plane-wave incidence the results may be put into the same form used by Ignatowsky and Zaziska.*

- - - - - - -

*Zaviska's work, although applicable to the problem of the finite grating has never been extended in this way. The form of the analysis to be presented in the next section is similar to Zaviska's though here the use of a Green's function formulation gives a clearer physical insight into the problem and leads naturally to a final form of the scattered field expression identical with Zaviska's.

Except for the work of Shaefer and Reiche[15] in 1911 no one has considered the problem of diffraction by a finite array of cylinders. As has been mentioned, their analysis neglected the coupling between grating elements so that for purposes of closely correlating theory and the possibilities of practical measurements there is need of an analysis which takes into account this coupling in a finite grating as well as the point (or line) nature of experimentally feasible sources of electromagnetic waves. It is the purpose of the succeeding section to develop such an analysis, which will relate closely to the physical situation of currents on the surface of the scattering elements.

2. Outline of the Theory.

In the following only scalar scattering by circular cylinders is considered since this results in a mathematically tractable problem although from Lamb's[2] work on the grating of closely spaced small wires or strips it is expected that for small scattering elements the precise form of their boundary is secondary in determining their scattered field in directions away from the source of radiation. The theory assumes a current distribution on the surface of each perfectly conducting cylinder; the total field is then calculated through the use of one of Green's theorems. Application of the boundary conditions gives a series of integral equations for the current on each cylinder which takes into account arbitrary excitation and coupling between all the elements. The unknown surface current on each cylinder is then expanded in a complex Fourier series whose coefficients may be evaluated using the usual orthogonality property of the trigonometric functions. The resulting system of linear algebraic equations in the unknown coefficients may be written as an infinite matrix equation. The problem then remaining is to solve this system of linear algebraic equations. Various methods of numerical solution may be used, depending on the number of terms and accuracy required in the final result. For small cylinders the terms off the principal diagonal are small, and the meaning of the term "small" may be evaluated readily in estimating the importance of higher-mode currents contributing to the scattered field. The results obtained at this point in the analysis are similar in form to those of Zaviska[17] who started by assuming a spectrum of scattered cylindrical waves and determining the spectral amplitudes from a consideration of the boundary conditions. There is also a formal analogy to the results of Twersky's[6, 21] multiple-order scattering analysis.

This theory is readily specialized to the case of a plane wave incident on an infinite planar grating of small wires. If the effects of higher-order current modes are neglected, this result becomes identical with that of Wessel[5] who considered a uniform current distribution on the surface of the wires in his analysis.

3. General Theory

Figure 1-1 shows the general arrangement of line source and scattering cylinders. The axes of the cylinders and line source are all parallel to the z-axis so that all relevant electromagnetic field quantities may be derived from the single scalar quantity E_z, the electric field intensity in the z-direction. For convenience in notation, define

$$E_z(x,y) = \psi(x,y) \quad .$$

Then from Maxwell's equations it is well known that in a source free region the scalar ψ must satisfy the wave equation

$$(\nabla^2{}_{x,y} + K^2)\psi(x,y) = 0 \quad ,$$

subject to the boundary condition, that ψ vanish on all perfectly conducting surfaces parallel to the z-direction. In addition, of course, the usual restriction on the form of the solution at infinity must be satisfied. The conventional harmonic time dependence $e^{-i\omega t}$ is used throughout with $K = 2\pi/\lambda$ where λ is the free-space wavelength.

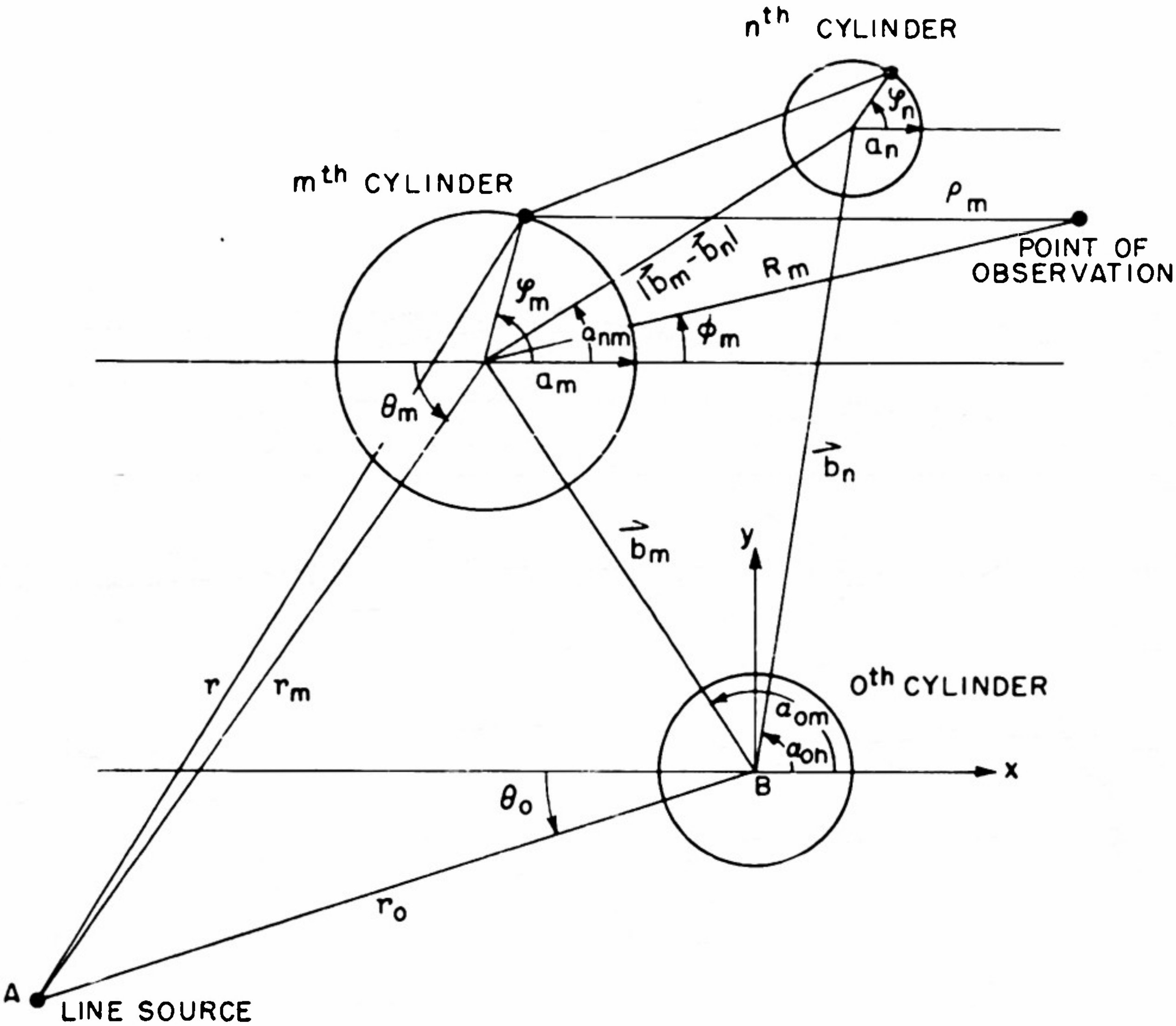

FIG. 1 GEOMETRY FOR SCATTERING FROM AN ARBITRARY ARRAY OF CYLINDERS

If a Green's function $(G(x,y;x',y')$ is defined as a solution of the inhomogeneous wave equation

$$(\nabla^2_{x,y} + K^2)/G(x,y;y',y') = -\delta(x-x')\delta(y-y') \quad ,$$

and substituted into Green's scalar identity

$$\int (\psi\nabla^2 G - G\nabla^2\psi)d\ ' = \oint (\psi\frac{\partial G}{\partial n} - G\frac{\partial \psi}{\partial n})dC' \ .$$

The result

$$\psi(x,y) = \oint (G\frac{\partial\psi}{\partial n} - \psi\frac{\partial G}{\partial n})dC'$$

is readily found, where the line integral is taken over a closed contour containing the source and all the cylinders. By imposing the boundary condition $\psi = 0$ on the surfaces of all cylinders and making the convenient definition

$$\left.\frac{\partial\psi}{\partial n}\right|_{\text{on nth cylinder}} = \frac{1}{2\pi a_n} I_n(\phi_n) \ ,$$

where $I_n(\phi_n)$ may be considered as the surface current on the nth cylinder, the previous result can be reduced to

$$\psi(\vec{r}) = \psi^{inc}(\vec{r}) + \frac{1}{2\pi}\sum_n \int_0^{2\pi} I_n(\phi_n)G(\vec{r},\vec{r}\,')d\phi_n \ , \qquad (1)$$

for r' on the surface of the cylinders, vector notation being used here as a convenience and $\psi^{inc}(r)$ is the field that would exist at the point r if no scattering obstacles were present.

The application of the boundary condition $\psi(r) = 0$ when r is on the surface of each cylinder leads to the following set of integral equations:

$$\left.\psi^{inc}(\vec{r})\right|_{\vec{r}\text{ on cylinders}} = -\frac{1}{2\pi}\sum_n \int_0^{2\pi} I_n(\phi_n)G(\vec{r},\vec{r}\,')d\phi_n \Bigg|_{\substack{\vec{r},\vec{r}\,'\text{ on}\\ \text{cylinders}}}$$

there is one such equation for each cylinder. Before proceeding to solve the unknown current distribution $I_n(\phi_n)$ on each cylinder, it is necessary to choose the appropriate Green's function. It is well known* that the two-dimensional Green's function which represents a radiating cylindrical wave in free space is

$$G(\vec{r},\vec{r}\,') = \frac{i}{4} H_0^{(1)}(K|\vec{r}-\vec{r}\,'|) \tag{2}$$

where $H_0^{(1)}(K|\vec{r}-\vec{r}\,'|)$ is the Hankel function of order zero.

The final form of the set of integral equations for the unknown surface-current distribution on each cylinder is thus

$$\psi^{inc}(\vec{r})\Big|_{\vec{r}\text{ on cylinder}} = -\frac{i}{8\pi}\sum_n \int_0^{2\pi} I_n(\phi_n) H_0^{(1)}(K|\vec{r}-\vec{r}\,'|)\,d\phi_n\Big|_{\substack{\vec{r},\vec{r}\,'\text{ on}\\ \text{cylinders}}} \tag{3}$$

The problem now is to find a set of $I_n(\phi_n)$ which satisfy this integral equation. One method of solving such an integral equation is to expand the unknown function in a complete set of orthonormal functions appropriate to the geometry of the particular problem and then to determine the resulting unknown coefficients. Following this method a natural choice here is to expand the surface current on each cylinder in the complex Fourier series

$$I_n(\phi_n) = \sum_{s=-\infty}^{\infty} a_{ns} e^{is\phi_n} .$$

Thus the solution of the integral equation is reduced to the problem of determining the a_{ns}. By assuming the $I_n(\phi_n)$ to have a sufficiently regular behavior, and by using the orthogonal properties of

- - - - - - -

*See for example Morse and Feshbach, "Methods of Theoretical Physics," (MIT notes) p. 155.

the set of functions $e^{is\phi_n}$, it is possible to reduce the problem of finding the a_{ns} to the solution of an infinite set of linear inhomogeneous simultaneous algebraic equations in which the a_{ns} are the unknowns.

If the mth integral equation is multiplied by $e^{-it\phi_m}$ (t is any integer including zero) and both sides are integrated with respect to ϕ_m from 0 to 2π, it follows that

$$\int_0^{2\pi} \psi^{inc}(\vec{r})\Big|_{\vec{r}\text{ on mth cylinder}} e^{-it\phi_m}\, d\phi_m =$$

$$-\frac{i}{8\pi}\sum_n\sum_s\int_0^{2\pi}\int_0^{2\pi} a_{ns}e^{is\phi_n} H_0^{(1)}(K|\vec{r}-\vec{r}\,'|)\Big|_{\substack{\vec{r}\text{ on mth cylinder}\\ \vec{r}\,'\text{ on mth and nth cylinder}}} e^{-it\phi_m} d\phi_n d\phi_m$$

Assuming that the order of integration and summation may be interchanged, and further introducing the notation

$$K_{tmns} = \frac{i}{8\pi}\int_0^{2\pi}\int_0^{2\pi} e^{is\phi_n} H_0^{(1)}(k|\vec{r}-\vec{r}\,'|)\Big|_{\substack{\vec{r}\text{ on mth cylinder}\\ \vec{r}\,'\text{ on mth and nth cylinder}}} e^{-it\phi_m}\, d\phi_n\, d\phi_m \tag{4}$$

and

$$Y_{tm} = \int_0^{2\pi} \psi^{inc}(\vec{r})\Big|_{\vec{r}\text{ on mth cylinder}} e^{-it\phi_m}\, d\phi_m$$

the equation for a_{ns} can be written

$$Y_{tm} = -\sum_n\sum_s K_{tmns}a_{na} \tag{5}$$

where t ranges over the same integers as s, and n ranges over all the cylinders.

Once the source excitation $\psi^{inc}(\vec{r})$ is specified the statement of the problem is complete and there remains the analytical problem of solving the linear equations (5) for the a_{ns}.

The incident field characteristic of a uniform line source is

$$\psi^{inc}(\vec{r}) = AH_o^{(1)}(K|\vec{r}|)$$

where A is an arbitrary complex constant. With this choice of excitation the integrals γ_{tm} and K_{tmns} as evaluated in Appendix B are

$$\gamma_{tm} = 2\pi AJ_t(Ka_m)H_t^{(1)}(K|\vec{r}_m|)e^{-it(\theta_m+\pi)}$$

$$K_{tmns} = \frac{\pi i}{2} J_t(Ka_m)\begin{cases} H_s^{(1)}(Ka_m)\ \delta_{st} & \Big|\ \vec{r}=\vec{r}' \text{ on mth cylinder} \\ J_s(Ka_n)H_{t-s}^{(1)}(K|\vec{b}_m-\vec{b}_n|)e^{-it\alpha_{nm}+is\alpha_{nm}} & \Big|\ \vec{r},\vec{r}' \text{ on different cylinders} \end{cases} \qquad (6)$$

For any given values of the parameters K, a_n, θ_m and $|\vec{b}_m-\vec{b}_n|$, γ_{tm} and K_{tmns} may be evaluated using existing tables of the Bessel functions. Finally, the total field from the array may be calculated readily using (1). Thus

$$\psi^{scatt} = \frac{i}{8\pi}\sum_n\sum_s a_{ns}\int_0^{2\pi} e^{is\phi_n} H_o^{(1)}(K\rho_n)d\phi_n$$

where as in Fig. 1

$$\rho_m = \sqrt{R_m^2 + a^2 - 2R_m a\cos(\phi_m-\theta_m)}$$

After substituting this last expression for ρ_m in the formula above, the integration may be performed through use of the addition theorem for Bessel functions* to give

- - - - - - -

*See Appendix A.

$$\psi^{tot}(x,y) = \psi^{inc}(x,y) + \frac{i}{4} \sum_n \sum_s a_{ns} J_s(Ka_n) H_s^{(1)}(KR_n) e^{is\phi_n} \qquad (7)$$

Here the reader familiar with Twersky's[6] multiple scattering analysis will notice a formal analogy between equation (7) and his formula for the scattered field.

At this point it is convenient to show the connection of this theory to the work of Wessel[5] on the infinite planar grating of cylindrical wires.

As the source is moved off to infinity, $\theta_m \longrightarrow \theta_o$

$$\psi^{inc} = AH_o^{(1)}(K|\vec{r}|) \sim A\sqrt{\frac{2}{\pi K r_o}}\, e^{iK|b_m| \cos(\theta_o - \alpha_{om})}$$

and

$$\psi^{inc}(\vec{r})\Big|_{\substack{\vec{r} \text{ on mth} \\ \text{cylinder}}} = AH_o^{(1)}(K|\vec{r}|) \sim A\sqrt{\frac{2}{\pi K r_o}} \cdot e^{iKr_o + iK|b_m|\cos(\theta_o - \alpha_{om}) + iKa_m\cos(\theta_o - \phi_m) - \frac{i\pi}{4}}$$

If A is chosen to make

$$\psi^{inc}(\vec{r})\Big|_{\vec{r} \text{ on mth cylinder}} = e^{iK|b_m|\cos(\theta_o - \alpha_{om}) + iKa_m\cos(\theta_o - \phi_m)}$$

corresponding to a plane wave incident from the direction θ_o then

$$\gamma_{tm} = 2\pi J_t(Ka_m) e^{iK|\vec{b}_m|\cos(\theta_o - \alpha_{om}) - it(\theta_o - \frac{\pi}{2})}, \qquad (8)$$

and for a planar array of equally spaced identical cylinders $|\vec{b}_m|$ $= mb$ (b is the distance between centers of adjacent cylinders),

$$\alpha_{om} = \begin{cases} \alpha_o \text{ for } m > 0 \\ \alpha_o \pm \pi \text{ for } m < 0 \end{cases}$$

$$a_m = a$$

From symmetry it is apparent that all the cylinders have the same current distribution except for the phase factor $e^{iKmb\cos(\theta_o-\alpha_o)}$. Thus

$$a_{ms} = e^{iKmb\cos(\theta_o-\alpha_o)} a'_{os} \tag{9}$$

where a'_{os} is the sth Fourier coefficient on the zeroth cylinder in the array. Thus, for this special case, equation (5) may be written as follows:

$$4ie^{-it(\theta_o-\frac{\pi}{2})} = H_t^{(1)}(Ka)a'_{ot} +$$

$$e^{-it\alpha_o} \sum_{\substack{n=-\infty \\ n\neq m}}^{\infty} \sum_{s=-\infty}^{\infty} a'_{os}\, e^{iK(n-m)b\cos(\theta_o-\alpha_o)}\, e^{is\alpha_o} J_s(Ka)H_{t-s}^{(1)}(K|n-m|b) \tag{10}$$

This equation is valid for all m. In particular, as stated above in (9), it is only necessary to calculate the current on the zeroth cylinder in order to know it on every cylinder. Thus, the system of equations for m = 0 becomes

$$4ie^{-it(\theta-\frac{\pi}{2})} = H_t^{(1)}(Ka)a'_{ot}$$

$$+ e^{-it\alpha_o} \sum_{\substack{n \\ n\neq 0}} \sum_{s} a'_{os} e^{iKnb\cos(\theta_o-\alpha_o)} e^{is\alpha_o} J_s(Ka)H_{t-s}^{(1)}(K|n|b)$$

As t ranges through all the integers from $-\infty$ to $+\infty$ an infinite number of equations in the infinite set of unknowns a'_{os} is generated. In principle, this set of equations could be solved for the a'_{os}. However, it is not proposed to do so at present. For small Ka and b >> a it may be seen from the behavior of the Bessel and Hankel functions involved that the dominant terms in the right-hand side of the previous expression are those with t = s = 0. Thus equation (10) becomes

$$41 = \left\{ H_0^{(1)}(Ka) + \sum_{\substack{n=-\infty \\ n\neq 0}}^{\infty} J_0(Ka) H_0^{(1)}(K|n|b) e^{iKnb\cos(\theta_0-\alpha_0)} \right\} a'_{00} \quad .$$

This is identical with the equation for the current on the zeroth cylinder obtained by Wessel. Tables of the series $\sum_{n=1}^{\infty} J_0(nKb)$ and $\sum Y_0(nKb)$ corresponding to normal incidence have been computed by Ignatowsky[12] and Wessel.[5]

As far as coupling effects and their dependence on cylinder radius and spacing are concerned, the mode coefficients could be computed with a large amount of labor for the case of an infinite planar grating using equation (10). However, when it comes to comparing the theoretical results for the scattered field to experimental results, it is not feasible to use plane-wave excitation, and the system of equations for the mode coefficients for a line source of excitation and the infinite grating are exceedingly complex. Hence, it is expedient to consider the simplest configuration for which mutual coupling effects may be calculated with a reasonable amount of labor. For these reasons the problem of scattering of a cylindrical wave by two identical cylinders has been chosen as an example to test the general theory.

4. Theory Specialized to the Case of Two Identical Cylinders

Arbitrary Incidence (Plane-wave excitation)

In view of the complexity of the general theory developed in the preceding section it is expedient to apply the theory to a simple problem which illustrates the effects of both the size and the separation of the elements in determining mutual interaction. The simplest configuration for such a study appears to be that of two identical cylinders arranged as in Fig. 2. To simplify further the equations determining the current distribution coefficients a_{ns} the incident field is assumed to be a plane wave, although for the case of normal incidence the equations will later be written down for a line source of primary excitation, since it is for this type of excitation that experimental measurements will be made.

Using the notation in Section 4, and starting from the general forms, Eq. 6, for the coefficients γ_{tm} and K_{tmns} with the substitutions $\theta_o = \theta_m = 0$, $\alpha_{01} = \pi/2 + \theta$ and $\alpha_{0-1} = -(\pi m/2 - \theta)$ as indicated in Fig. 2, the following expressions are obtained for plane-wave incidence:

$$\left.\begin{aligned} \gamma_{tm} &= 2\pi J_t(Ka)e^{\mp iKb\sin\theta + it\frac{\pi}{2}} \\ K_{tmns} &= \frac{\pi i}{2}\begin{Bmatrix} H_s^{(1)}(Ka)\,\delta_{st} \\ J_s(Ka)H_{t-s}^{(1)}(2Kb) \quad e^{-it(\theta \pm \frac{\pi}{2}) + is(\theta \pm \frac{\pi}{2})} \end{Bmatrix} \end{aligned}\right\} \qquad (11)$$

The upper sign in the exponents is used for m = 1 and the lower sign for m = -1. When the above expressions for γ_{tm} and K_{tmns} are substituted in equation (5), the linear equation for the unknowns a_{ns} are for m = 1:

$$H_t^{(1)}(Ka)a_{1,t} + e^{-it(\theta - \frac{\pi}{2})}\Bigg\{J_o(Ka)H_t^{(1)}(2Kb)a_{-1,0} \qquad (12)$$

$$+ \sum_{s=1}^{\infty} e^{-is\frac{\pi}{2}} J_s(Ka)\left[e^{is\theta}H_{t-s}^{(1)}(2Kb)a_{-1,s} + e^{-is\theta}H_{t+s}^{(1)}(2Kb)a_{-1,-s}\right]\Bigg\}$$

$$= 4ie^{-iKb\sin\theta + it\frac{\pi}{2}}$$

and for m = -1:

$$H_t^{(1)}(Ka)a_{-1,t} + e^{-it(\theta + \frac{\pi}{2})}\Bigg\{J_o(Ka)H_t^{(1)}(2Kb)a_{1,0} \qquad +$$

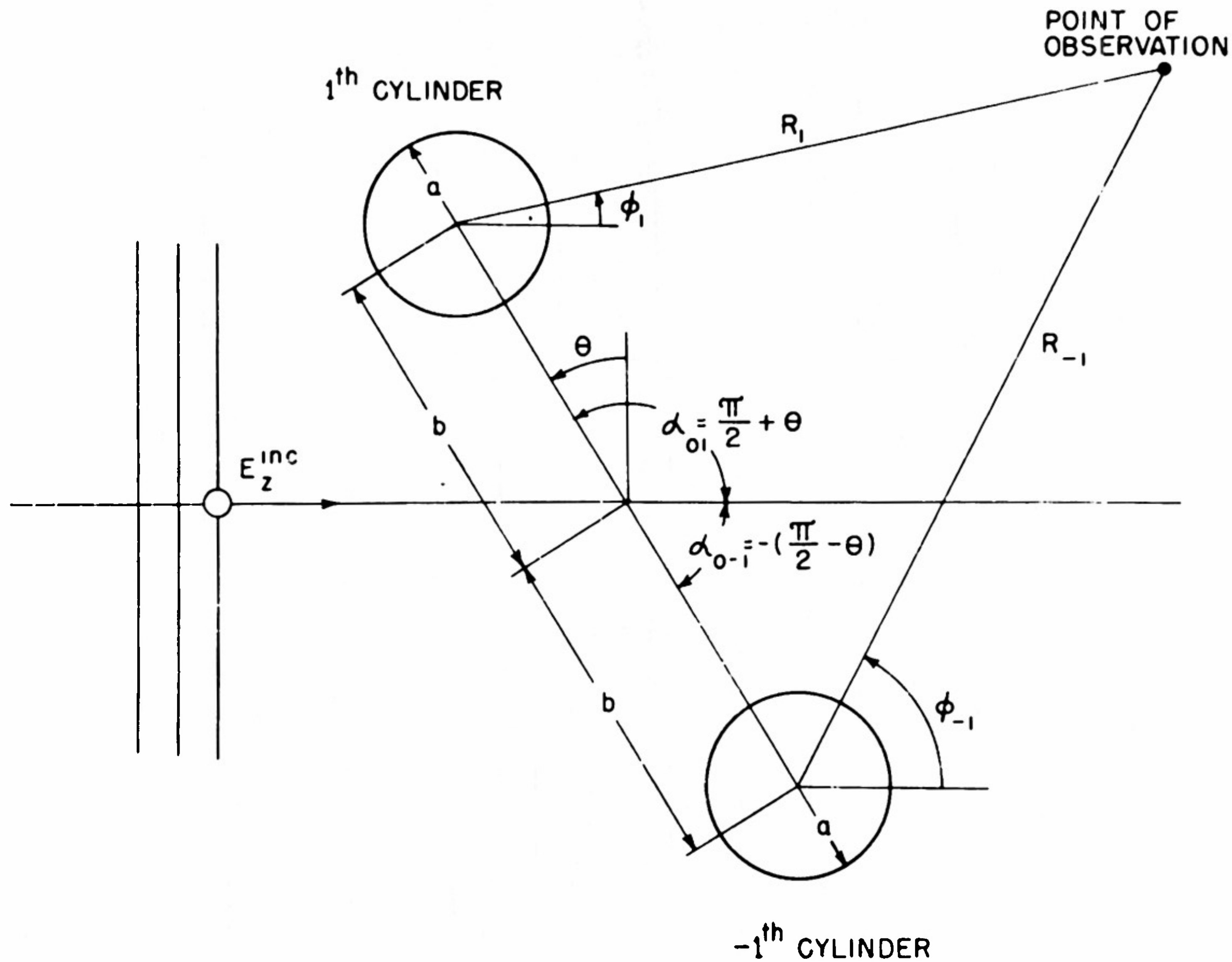

FIG. 2 GEOMETRY FOR SCATTERING OF A PLANE WAVE BY TWO IDENTICAL CYLINDERS (ARBITRARY ANGLE OF INCIDENCE)

$$+\sum_{s=1}^{\infty} e^{is\frac{\pi}{2}} J_s(Ka)\left[e^{is\theta}H^{(1)}_{t-s}(2Kb)a_{1,s} + e^{-is\theta}H^{(1)}_{t+s}(2Kb)a_{1,-s}\right]$$

$$= 4ie^{iKb\sin\theta + it\frac{\pi}{2}} \tag{13}$$

The system of equations (12) and (13) may be studied conveniently if they are written out in detail for a number of values of the index t, and then gathered together in matrix form. For convenience, the matrix form is $K \cdot a = 4ie^{+iKb\sin\theta}\lambda$ where the square matrix K is the matrix of coefficients of the unknowns $a_{\pm 1,s}$ on the left-hand side of (12) and (13), a is the column matrix of the unknowns $a_{\pm 1,s}$, and λ is the column matrix of the elements $e^{it\pi/2}$ on the right-hand side of (12) and (13). This procedure has been followed in setting up the matrix equation shown in Fig. 2 where the indices t and s run from -2 to +2.

In writing a finite matrix equation in place of the infinite matrix equation required by the rigorous theory the effect of neglecting all equations with $|t|$ and $|s|$ ranging from a given integer to infinity (in this case the equations with t and s ranging from $\pm$ 3 to $\pm$ ∞ have been neglected) must be determined. In general it is difficult to justify rigorously the neglect of 'higher-order' equations. However, in this particular problem the known behavior of the cylinder functions which comprise the coefficients permits a heuristic justification of the neglect of such 'higher-order' equations. This justification is treated in detail later and for the present the validity of the solutions obtained from the finite matrix equation will be assumed.

For a spacing that is much larger than the cylinder radius, it is apparent from the behavior of the coefficients* in the matrix equation as written in Fig. 3 that the predominant elements in the K matrix lie along the two principal diagonals, that is, the diagonals running from the upper-left-hand to the lower-right-hand corners, and from the upper-right-hand to the lower-left-hand corners. The degree of approximation involved in the use of these terms alone in solving the finite system of equations will be discussed later. For present purposes useful information about the behavior of the far-zone field may be derived from the matrix equation by assuming this approximation to be good. In essence this assumption means that the current distribution in each mode (characterized by the indices $\pm s$) is independent of the current distribution in other modes.

For example, from the matrix equation in Fig. 3 the zeroth-mode coefficients $a_{\pm 1,0}$ will be determined from the pair of equations

- - - - - - -

*For small Ka

$$J_n(Ka) \simeq \left(\frac{Ka}{2}\right)^n \frac{1}{n!}$$

$$H_n^{(1)}(Ka) \simeq - \frac{i(n-1)!}{\pi} \left(\frac{2}{Ka}\right)^n \quad \text{for } n \neq 0$$

$$\simeq - \frac{2i}{\pi} \ln \frac{2i}{\gamma Ka} \quad \text{for } n = 0$$

and for large Kb

$$H_n^{(1)}(kb) \simeq \sqrt{\frac{2}{\pi Kb}}\, e^{i\left(Kb - \frac{in\pi}{2} - \frac{i\pi}{4}\right)} \quad \text{for } Kb >> n$$

These expressions are useful in studying the behavior of the K matrix elements for small Ka and large Kb. A detailed discussion of the behavior of the elements as depends on order n, and the magnitudes of Ka and Kb will be found later.

$$
\begin{array}{ll}
\begin{array}{r} \\ \\ m=1 \\ \\ \\ \\ \\ m=-1 \\ \\ \\ \end{array}
\begin{array}{c} t=-2 \\ t=-1 \\ t=0 \\ t=1 \\ t=2 \\ t=-2 \\ t=-1 \\ t=0 \\ t=1 \\ t=2 \end{array}
&
\left[\begin{array}{cccccccccc}
H_2^{(1)}(ka) & 0 & 0 & 0 & 0 & J_2(ka)H_0^{(1)}(2kb) & -ie^{i\theta}J_1(ka)H_1(2kb) & -e^{2i\theta}J_0(ka)H_2^{(1)}(2kb) & ie^{3i\theta}J_1(ka)H_3^{(1)}(2kb) & e^{4i\theta}J_2(ka)H_4^{(1)}(2kb) \\
0 & -H_1^{(1)}(ka) & 0 & 0 & 0 & ie^{-i\theta}J_2(ka)H_1^{(1)}(2kb) & -J_1(ka)H_0^{(1)}(2kb) & ie^{i\theta}J_0(ka)H_1(2kb) & -e^{2i\theta}J_1(ka)H_2(2kb) & -ie^{3i\theta}J_2(ka)H_3(2kb) \\
0 & 0 & H_0^{(1)}(ka) & 0 & 0 & -e^{-2i\theta}J_2(ka)H_2^{(1)}(2kb) & -ie^{-i\theta}J_1(ka)H_1^{(1)}(2kb) & J_0(ka)H_0^{(1)}(2kb) & ie^{i\theta}J_1(ka)H_1^{(1)}(2kb) & -e^{2i\theta}J_2(ka)H_2^{(1)}(2kb) \\
0 & 0 & 0 & H_1^{(1)}(ka) & 0 & -ie^{-3i\theta}J_2(ka)H_3^{(1)}(2kb) & e^{-2i\theta}J_1(ka)H_2^{(1)}(2kb) & ie^{-i\theta}J_0(ka)H_1^{(1)}(2kb) & J_1(ka)H_0^{(1)}(2kb) & -ie^{i\theta}J_2(ka)H_1^{(1)}(2kb) \\
0 & 0 & 0 & 0 & H_2^{(1)}(ka) & e^{-4i\theta}J_2(ka)H_4^{(1)}(2kb) & ie^{-3i\theta}J_1(ka)H_3^{(1)}(2kb) & -e^{-2i\theta}J_0(ka)H_2^{(1)}(2kb) & -ie^{-i\theta}J_1(ka)H_1^{(1)}(2kb) & J_2(ka)H_0^{(1)}(2kb) \\
J_2(ka)H_0^{(1)}(2kb) & ie^{i\theta}J_1(ka)H_1^{(1)}(2kb) & -e^{2i\theta}J_0(ka)H_2^{(1)}(2kb) & -ie^{3i\theta}J_1(ka)H_3^{(1)}(2kb) & e^{4i\theta}J_2(ka)H_4^{(1)}(2kb) & H_2^{(1)}(ka) & 0 & 0 & 0 & 0 \\
-ie^{-i\theta}J_2(ka)H_1^{(1)}(2kb) & -J_1(ka)H_0^{(1)}(2kb) & -ie^{i\theta}J_0(ka)H_1^{(1)}(2kb) & -e^{2i\theta}J_1(ka)H_2^{(1)}(2kb) & ie^{3i\theta}J_2(ka)H_3^{(1)}(2kb) & 0 & -H_1^{(1)}(ka) & 0 & 0 & 0 \\
-e^{-2i\theta}J_2(ka)H_2^{(1)}(2kb) & ie^{-i\theta}J_1(ka)H_1^{(1)}(2kb) & J_0(ka)H_0^{(1)}(2kb) & -ie^{i\theta}J_1(ka)H_1^{(1)}(2kb) & -e^{2i\theta}J_2(ka)H_2^{(1)}(2kb) & 0 & 0 & H_0^{(1)}(ka) & 0 & 0 \\
ie^{-3i\theta}J_2(ka)H_3^{(1)}(2kb) & e^{-2i\theta}J_1(ka)H_2^{(1)}(2kb) & -ie^{-i\theta}J_0(ka)H_1^{(1)}(2kb) & J_1(ka)H_0^{(1)}(2kb) & -ie^{i\theta}J_2(ka)H_1^{(1)}(2kb) & 0 & 0 & 0 & H_1^{(1)}(ka) & 0 \\
e^{-4i\theta}J_2(ka)H_4^{(1)}(2kb) & -ie^{-3i\theta}J_1(ka)H_3^{(1)}(2kb) & -e^{-2i\theta}J_0(ka)H_2^{(1)}(2kb) & -ie^{-i\theta}J_1(ka)H_1^{(1)}(2kb) & J_2(ka)H_0^{(1)}(2kb) & 0 & 0 & 0 & 0 & H_2^{(1)}(ka)
\end{array}\right]
\cdot
\left[\begin{array}{c} a_{1,-2} \\ a_{1,-1} \\ a_{1,0} \\ a_{1,1} \\ a_{1,2} \\ a_{-1,-2} \\ a_{-1,-1} \\ a_{-1,0} \\ a_{-1,1} \\ a_{-1,2} \end{array}\right]
= 4i
\left[\begin{array}{c} e^{-ikb\sin\theta}\left\{\begin{array}{c} -1 \\ -i \\ 1 \\ i \\ -1 \end{array}\right\} \\ e^{ikb\sin\theta}\left\{\begin{array}{c} 1 \\ -i \\ 1 \\ i \\ -1 \end{array}\right\} \end{array}\right]
\end{array}
$$

FIG. 3. THE MATRIX EQUATION $K \cdot a = 4ie^{\pm ikb\sin\theta}\lambda$, FOR THE SCATTERING OF A PLANE WAVE BY TWO IDENTICAL PERFECTLY CONDUCTING CYLINDERS INDEX t RANGING FROM -2 TO $+2$.

$$H_o^{(1)}(Ka)a_{1,0} + J_o(Ka)H_o^{(1)}(2Kb)a_{-1,0} = 4ie^{-iKbsin\theta}$$

$$J_o(Ka)H_o^{(1)}(2Kb)a_{1,0} + H_o^{(1)}(Ka)a_{1,0} = 4ie^{\ iKbsin\theta}$$

The solutions to these are,

$$\begin{Bmatrix} a_{1,0} \\ a_{-1,0} \end{Bmatrix} = \frac{4i}{H_o^{(1)^2}(Ka) - J_o^2(Ka)H_o^{(1)^2}(2Kb)}$$

$$\begin{Bmatrix} H_o^{(1)}(Ka)e^{-iKbsin\theta} - J_o(Ka)H_o^{(1)}(2Kb)e^{iKbsin\theta} \\ H_o^{(1)}(Ka)e^{iKbsin\theta} - J_o(Ka)H_o^{(1)}(2Kb)e^{-iKbsin\theta} \end{Bmatrix}$$

Similar expressions are obtained for the other-mode coefficients $a_{\pm 1,+s}$, and in general they may be written in the following form:

$$\begin{Bmatrix} a_{1,\pm s} \\ a_{-1,\pm s} \end{Bmatrix} = \frac{4ie^{\frac{\pi i}{2}s}}{H_s^{(1)^2}(Ka) - J_s^2(Ka)H_{2s}^{(1)^2}(2Kb)}.$$

$$\begin{Bmatrix} H_s^{(1)}(Ka)e^{-iKbsin\theta} - J_s(Ka)H_{2s}^{(1)}(2Kb)e^{\ iKbsin\theta-2is\theta} \\ H_s^{(1)}(Ka)e^{iKbsin\theta} - J_s(Ka)H_2^{(1)}(2Kb)e^{-iKbsin\theta-2is\theta} \end{Bmatrix} \qquad (14)$$

Equation (7) (repeated here for convenience)

$$\psi^{tot}(x,y) = \psi^{inc}(x,y) + \frac{i}{4} \sum_n \sum_e a_{ns}J_s(Ka)H_s^{(1)}(KR_n)e^{is\phi_n} \qquad (15)$$

can be used to calculate the total field. However, the terms $H_s^{(1)}(KR_n)e^{is\phi_n}$ in the summation for the scattered field are complicated functions of the position of the point of observation, so for simplicity the point of observation will be taken in the far zone, along the line of the incident wave direction. This means that $\phi_{+1} \sim 0$, and $R_{+1} \sim R_o \pm b\sin\theta$, so the well known asymptotic form of the Hankel functions for argument KR_o much greater than the order s gives,

$$H_s^{(1)}(KR_{\pm 1}) \simeq \frac{e^{-i\pi/4}}{\pi}\sqrt{\frac{\lambda}{R_o}}\, e^{\pm iKb\sin\theta}$$

With these simplifications the part of equation (15) representing the scattered field becomes

$$\psi^{scatt} \simeq \frac{1}{4\pi}\, e^{iKR_o - i\pi/4}\sqrt{\frac{\lambda}{R_o}} \sum_{n=\pm 1} e^{\pm iKb\sin\theta}\Big(a_{no}J_o(Ka) + \sum_{s=1}^{\infty} e^{-is\pi/2} J_s(Ka)(a_{n,s} + a_{n-s})\Big)$$

From (14) the terms $(a_{n,s}+a_{n-s})$ may be combined (for $n = \pm 1$) as,

$$a_{\pm 1,s}+a_{\pm 1,-s} = \frac{4ie^{\frac{\pi i}{2}|s|}}{H_s^{(1)2}(Ka) - J_s^2(Ka)H_2^{(1)2}(2Kb)}\Big(H_s^{(1)}(Ka)e^{\mp iKb\sin\theta}$$

$$= J_s(Ka)H_{2s}^{(1)}(2Kb)\cos 2s\theta\; e^{\pm iKb\sin\theta}\Big)$$

Substitution of this last expression in equation (15) results in the following expression for the scattered field.

$$\psi^{scatt}(R_o) \simeq -\frac{\sqrt{2}\, e^{iKR_o - i\pi/4}}{\pi}\sqrt{\frac{2\lambda}{R_o}} \sum_{s=o}^{\infty} \varepsilon_s \frac{J_s(Ka)}{H_s^{(1)^2}(ka) - J_s^2(Ka) H_{2s}^{(1)^2}(2Kb)} \cdot$$

$$(H_s^{(1)}(Ka) - J_s(Ka) H_{2s}^{(1)}(2Kb)\cos 2s\theta \cos(2Kb\sin\theta)) \qquad (16)$$

From this result it is apparent that as the spacing between the cylinders becomes very large the scattered field shows negligible dependence on the angle of orientation of the plane of the cylinders in the incident wave-front. However, for moderately close coupling it is interesting to see the effect of orientation on the scattered field.

A comparison between the results of the above analysis and near-zone field measurements described in Section 5 for normal incidence with $2b/\lambda = 1$ shows that the theory which neglects the off-diagonal terms in the matrix equation gives reasonable results for Ka as large as 1.5. Therefore equation (16) has been used to calculate the far-zone form of the total field from the relation $\psi^{tot} = \psi^{inc} + \psi^{scatt}$ as a function of the angle θ. For convenience the factor $\frac{1}{\pi}\sqrt{\frac{2\lambda}{R_o}}$ has been chosen equal to 1/2, although for actual observation in the far zone, R_o/λ must be large and the above factor quite small. In Fig. 4 the amplitude of ψ^{tot} is (plotted as $|E_{z_{norm}}|$) shown as a function of θ for two cylinder radii corresponding to Ka = 0.10 and Ka = 1.50 with the spacing $2b/\lambda = 1.0$. In addition, the same quantity is plotted for the case where coupling is neglected.

From these results it is apparent that coupling effects (as evidenced by the difference between the curves with and without coupling) are considerably less dependent on the angle of orientation for the smaller than for the larger cylinder. In the case of the larger cylinder the coupling effects are slightly larger for normal incidence (i.e., $\theta = 0$) than for any other angle. This is not true for the small cylinder, but at least it is safe to assume that coupling effects are about as large at normal incidence as for any other angle of orientation for cylinders with Ka less than 1.5. The analysis presented above is only strictly true for spacing much larger than the radius. How much larger is a rather difficult question to answer, since it requires in effect the solution of the complete matrix equation, or an appeal to experiment. For the case discussed above b/a equaled approximately 2.1; but it is dangerous to use this ratio as a criterion for the range of validity of the approximation, since the off-diagonal elements in the K matrix are not related to the diagonal elements through any such simple algebraic function as b/a. Therefore the question of the useful range of approximation will be investigated experimentally in Section 5. Suffice it to say here that provided b is kept large enough the predictions of this theory should be in reasonable agreement with the actual situation for cylinders with Ka even greater than 1.5. It seems reasonable to assume that for cylinders with Ka even larger than 1.5 the effects of coupling should be about as large for normal incidence as for any other angles of orientation showing significant departures from the results based on the assumption of independent scattering. For this reason, and the additional fact that it would be exceedingly laborious to solve the matrix equation by numerical method for arbitrary orientation and cylinders with tighter coupling than assumed in the above example, the remainder of this chapter and succeeding chapters will consider only the case of normal incidence corresponding to θ equal to zero.

Normal Incidence

For normal incidence the effect of substituting a line source(or cylindrical wave) in place of the plane-wave excitation assumed previously presents no special difficulties because, as is apparent from the geometrical arrangement of the source and cylinders shown in Fig. 5, both cylinders are excited symmetrically. The system of equations (13) for the unknowns $a_{\pm 1,s}$ for m = -1 may be written

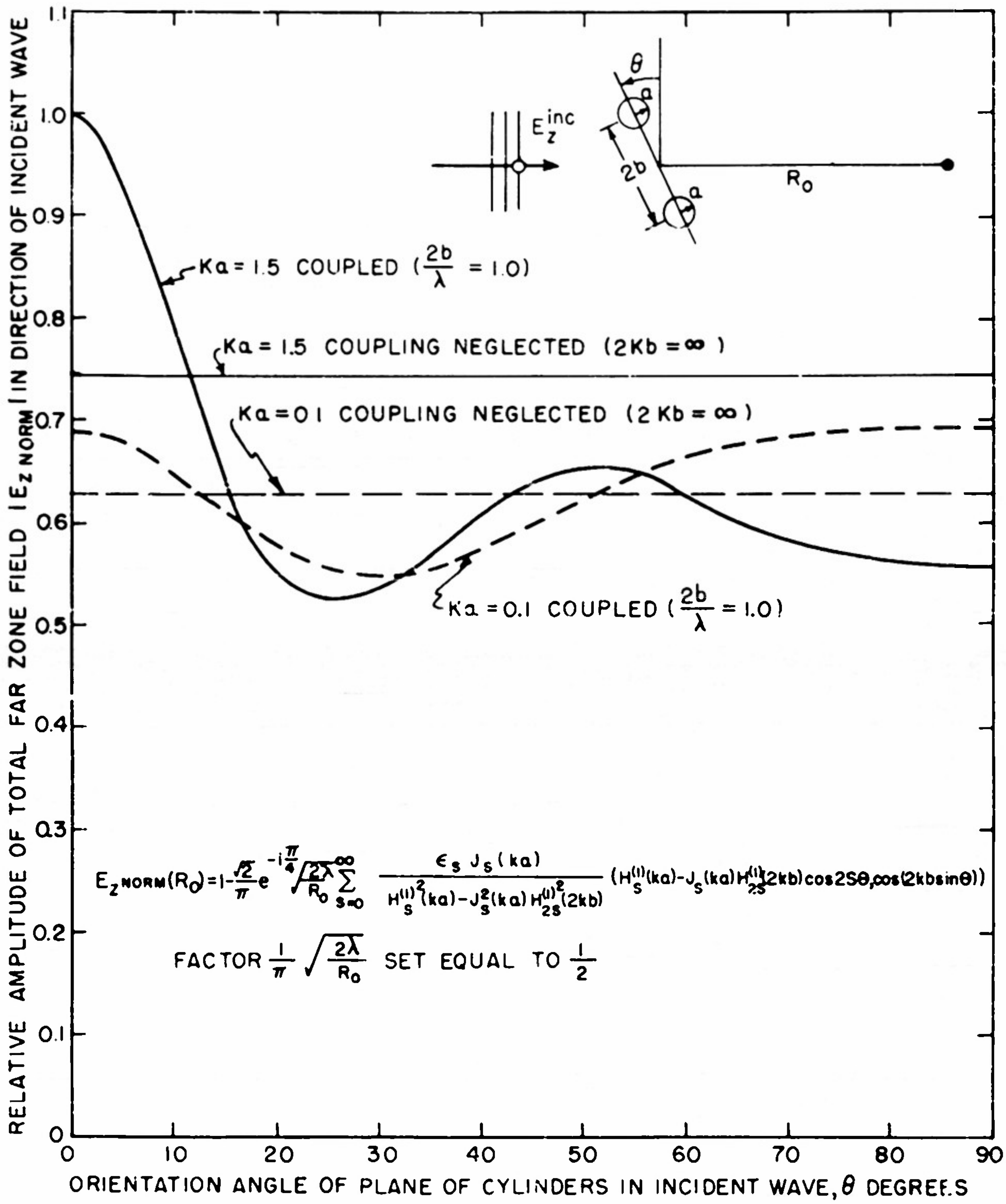

FIG. 4 APPROXIMATE THEORETICAL FAR ZONE FIELD IN DIRECTION OF INCIDENT WAVE FOR SCATTERING BY TWO IDENTICAL PERFECTLY CONDUCTING CYLINDERS, AS A FUNCTION OF ORIENTATION IN THE INCIDENT WAVE, FOR $Ka = 0.1$ AND $Ka = 1.5$ AND $\frac{2b}{\lambda} = 1.0$

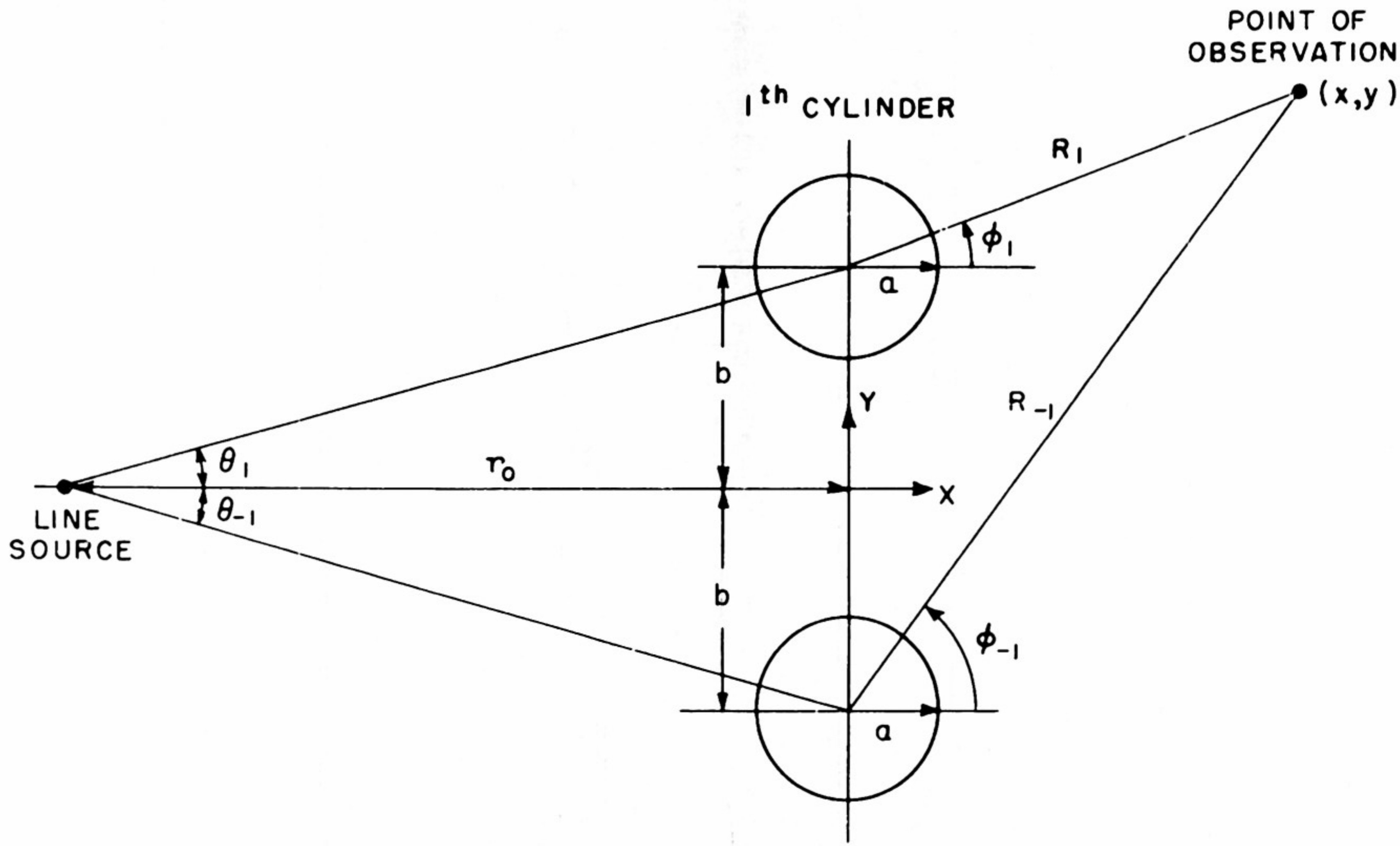

FIG. 5 GEOMETRY FOR SCATTERING FROM TWO IDENTICAL CYLINDERS (NORMAL INCIDENCE)

$$H_t^{(1)}(Ka)a_{-1,t} + e^{-it\pi/2}\Bigg\{ J_o(Ka)H_t^{(1)}(2Kb)a_{1,0} + \sum_{s=1}^{\infty} e^{is\pi/2} J_s(Ka)\Big[H_{t+s}^{(1)}(2Kb)a_{1,-s} + H_{t-s}^{(1)}(2Kb)a_{1,s}\Big]\Bigg\} = 4iH_t^{(1)}(K\sqrt{r_o^2+b^2})e^{-it(\pi+\theta_{-1})} \quad (17)$$

where the term $4iH_t^{(1)}(K\sqrt{r_o^2+b^2})e^{-it(\pi+\theta_{-1})}$ appearing on the right-hand-side differs from that in (12) because of the use of the γ_{tm} (see Eq. (6)) proper for line source excitation, rather than that for a plane wave.

If the angle θ is set equal to zero in the matrix equation, $K \cdot a = 4ie^{+iKbsin\theta}\lambda$ of Fig. 3 it is apparent that the equations for $m = 1$ and $m = -1$ are identical except that $a_{-1,s}$ must be replaced by $a_{1,-s}$ wherever it appears. This of course reduces by half the number of unknown coefficients to be determined, and is to be expected from the symmetry of the source and cylinders.

It is evident

$$I_1(\phi_1) = I_{-1}(-\phi_1)$$

where $I_1(\phi_1)$ and $I_{-1}(-\phi_1)$ are the surface currents at mirror image points on the upper and lower cylinders. If the Fourier representation

$$I_n(\phi_n) = \sum_s a_{ns}e^{is\phi_n}$$

is substituted into the above symmetry relationship the following identity is readily established,

$$a_{1,s} = a_{-1,-s}$$

for all s.

The system of equations relating the unknowns obtained from (7) by using this statement of symmetry and allowing t to range through all positive and negative integers may be conveniently summarized in matrix form as,

$$K \cdot a = 4i\lambda$$

where K is a square matrix, whose elements are the coefficients of the a_{1+s} and $4i\lambda$ is the matrix of elements on the right-hand-side of (17). This matrix equation has been written out explicitly in Fig. 6 for the index t ranging from -3 to +3.

The rigorous solution of the problem requires the solution of an infinite matrix equation. Except for certain special cases (in this problem, corresponding to no coupling, i.e. $Kb \rightarrow \infty$) the solution to such an infinite matrix equation is not immediately obvious, and indeed a simple solution may not exist at all.

An Approximation

The best that can be done by way of a solution is to solve by numerical means a finite number of the equations represented by (17). This procedure may be justified qualitatively in the following way. Firstly the elements on the principal diagonal in the K matrix of Fig. 6 are $H_t^{(1)}(ka) + J_1(Ka)H_{2t}^{(1)}(2Kb)$. (For t a negative integer multiply this expression by $e^{\pm\pi i t}$.) For large order (t being taken positive) t and the arguments Ka and 2Kb less than the order, use of the representations,*

$$\begin{matrix} J_t(t \operatorname{sech} \alpha) \\ Y_t(t \operatorname{sech} \alpha) \end{matrix} \simeq \pm \frac{e^{\pm t(\tanh\alpha - \alpha)}}{\sqrt{2\pi t \tanh\alpha}}$$

with the definition $\operatorname{sech} \alpha = Ka/t$ or Kb/t gives

$$H_t^{(1)}(Ka) + J_t(Ka)H_{2t}^{(1)}(2Kb)$$

$$\simeq \frac{1}{\sqrt{2\pi t\sqrt{1-(\frac{Ka}{t})^2}}}\left\{ e^{\cdot t(\operatorname{sech}^{-1}\frac{Ka}{t} - \sqrt{1-(\frac{Ka}{t})^2})} \right.$$

* - - - - - - -
See General Bibliography, Watson's "Bessel Functions," p. 243.

$$
\begin{array}{c}
t=-3 \\ t=-2 \\ t=-1 \\ t=0 \\ t=1 \\ t=2 \\ t=3
\end{array}
\left[\begin{array}{ccccccc}
-H_3^{(1)}(ka)-J_3(ka)H_6^{(1)}(2kb) & -iJ_2(ka)H_5^{(1)}(2kb) & J_1(ka)H_4^{(1)}(2kb) & iJ_0(ka)H_3^{(1)}(2kb) & J_1(ka)H_2^{(1)}(2kb) & -iJ_2(ka)H_1^{(1)}(2kb) & -J_3(ka)H_0^{(1)}(2kb) \\
-iJ_3(ka)H_5^{(1)}(2kb) & H_2^{(1)}(ka)+J_2(ka)H_4^{(1)}(2kb) & iJ_1(ka)H_3^{(1)}(2kb) & -J_0(ka)H_2^{(1)}(2kb) & iJ_1(ka)H_1^{(1)}(2kb) & J_2(ka)H_0^{(1)}(2kb) & iJ_3(ka)H_1^{(1)}(2kb) \\
J_3(ka)H_4^{(1)}(2kb) & iJ_2(ka)H_3^{(1)}(2kb) & -H_1^{(1)}(ka)-J_1(ka)H_2^{(1)}(2kb) & -iJ_0(ka)H_1^{(1)}(2kb) & -J_1(ka)H_0^{(1)}(2kb) & -iJ_2(ka)H_1^{(1)}(2kb) & J_3(ka)H_2^{(1)}(2kb) \\
iJ_3(ka)H_3^{(1)}(2kb) & -J_2(ka)H_2^{(1)}(2kb) & -iJ_1(ka)H_1^{(1)}(2kb) & H_0^{(1)}(ka)+J_0(ka)H_0^{(1)}(2kb) & iJ_1(ka)H_1^{(1)}(2kb) & -J_2(ka)H_2^{(1)}(2kb) & -iJ_3(ka)H_3^{(1)}(2kb) \\
-J_3(ka)H_2^{(1)}(2kb) & -iJ_2(ka)H_1^{(1)}(2kb) & -J_1(ka)H_0^{(1)}(2kb) & -iJ_0(ka)H_1^{(1)}(2kb) & H_1^{(1)}(ka)+J_1(ka)H_2^{(1)}(2kb) & iJ_2(ka)H_3^{(1)}(2kb) & -J_3(ka)H_4^{(1)}(2kb) \\
-iJ_3(ka)H_1^{(1)}(2kb) & J_2(ka)H_0^{(1)}(2kb) & -iJ_1(ka)H_1^{(1)}(2kb) & -J_0(ka)H_2^{(1)}(2kb) & -iJ_1(ka)H_3^{(1)}(2kb) & H_2^{(1)}(ka)+J_2(ka)H_4^{(1)}(2kb) & iJ_3(ka)H_5^{(1)}(2kb) \\
J_3(ka)H_0^{(1)}(2kb) & -iJ_2(ka)H_1^{(1)}(2kb) & -J_1(ka)H_2^{(1)}(2kb) & iJ_0(ka)H_3^{(1)}(2kb) & -J_1(ka)H_4^{(1)}(2kb) & -iJ_2(ka)H_5^{(1)}(2kb) & H_3^{(1)}(ka)+J_3(ka)H_6^{(1)}(2kb)
\end{array}\right]
\times
\left[\begin{array}{c}
a_{l,3} \\ a_{l,2} \\ a_{l,1} \\ a_{l,0} \\ a_{l,-1} \\ a_{l,-2} \\ a_{l,-3}
\end{array}\right]
= 4i
\left[\begin{array}{c}
H_3^{(1)}(K\sqrt{r_0^2+b^2})e^{-i3\theta} \\
H_2^{(1)}(K\sqrt{r_0^2+b^2})e^{-i2\theta} \\
H_1^{(1)}(K\sqrt{r_0^2+b^2})e^{-i\theta} \\
H_0^{(1)}(K\sqrt{r_0^2+b^2}) \\
H_1^{(1)}(K\sqrt{r_0^2+b^2})e^{i\theta} \\
H_2^{(1)}(K\sqrt{r_0^2+b^2})e^{i2\theta} \\
-H_3^{(1)}(K\sqrt{r_0^2+b^2})e^{i3\theta}
\end{array}\right]
$$

FIG. 6 THE MATRIX EQUATION $K \cdot a = 4i\lambda$ FOR FOURIER COEFFICIENTS ON lth CYLINDER IN TWO CYLINDER PROBLEM. t RANGING FROM -3 TO $+3$ (NORMAL INCIDENCE)

$$- ie^{t(\text{sech}^{-1}\frac{Ka}{t} - \sqrt{1-(\frac{Ka}{t})^2})}$$

$$+ \frac{e^{-t(\text{sech}^{-1}(\frac{Ka}{t}) - \sqrt{1-(\frac{Ka}{t})^2})}}{\sqrt{2\pi t}\ \sqrt{1-(\frac{Kb}{t})^2}} \left\{ \left[e^{-2t(\text{sech}^{-1}\frac{Kb}{t} - \sqrt{1-(\frac{Kb}{t})^2}} \right. \right.$$

$$\left. \left. -ie^{2t(\text{sech}^{-1}\frac{Kb}{t} - \sqrt{1-(\frac{Kb}{t})^2})} \right] \right\}$$

For $s >> Kb$, Ka; and Ka, $Kb >> 1$, several approximations may be made and this formula simplified to

$$\frac{-i}{\sqrt{2\pi t}} \left\{ (\frac{2t}{Ka})^t + \frac{1}{\sqrt{2\pi t}} \quad (\frac{2t}{Kb})^t \ (\frac{a}{b}) \ ^t \right\} \tag{18}$$

Thus the diagonal terms tend to become very large with increasing order. If the off-diagonal elements tend to become very small with increasing order then the procedure of solving only a finite number of the equations appears as reasonable. This is indeed true as is readily seen from the fact that the off-diagonal elements are of the form

$$J_s(Ka)H_{t-s}(2Kb) \quad (\text{for } s \neq t)$$

and that for large s (also $s >> Ka$, $2Kb$, and Ka, $Kb >>1$) this combination behaves as

$$\frac{1}{\sqrt{s}}(\frac{2s}{Ka})^{-|s|} \quad \frac{1}{\sqrt{t-s}} \ (\frac{t-s}{Kb})^{|t-s|}$$

Thus for s much larger than t this combination behaves essentially as

$$\frac{1}{|s|} \ \frac{1}{2^{|s|}} \ (\frac{a}{b})^{|s|} \ (\frac{Kb}{|s|})^{|t|}$$

which tends to zero with increasing s. This argument indicates that the approximation involved in choosing for solution only a finite number of the equations and unknowns represented in the infinite matrix equation is a very reasonable one.

Granted that the approximation is good, how many, and which equations should be chosen for solution? Since the problem of scattering by two cylinders must reduce to that of scattering by a single cylinder in the limit of very large spacing between cylinders, the first question is most readily answered by using the simple well-known solution to the problem of the scattering of a plane wave by an isolated cylinder. The symmetry of the diagonal elements of the K matrix about the element corresponding to $t = s = 0$ points to an obvious choice of equations as those with $t = 0, \pm 1, \pm 2 \ldots \pm n$, and unknowns with s ranging from $-n$ to $+n$. The scattered field (for the same orientation of the incident plane wave as in the two-cylinder problem from an isolated cylinder[22] may be put in the form

$$\psi^{scatt}(r,\phi) = -\sum_{s=0}^{\infty} \varepsilon_s i^{s+1} \sin \delta_s(Ka) e^{-i\delta_s(Ka)} H_s^{(1)}(Kr) \cos s\phi$$

where

$$H_s^{(1)}(Ka) = -iC_s(Ka) e^{i\delta_s(Ka)} \quad \text{and} \quad \varepsilon_s = \begin{cases} 1, & s = 0 \\ 2, & s \neq 0 \end{cases}$$

In the far zone the amplitude of $H_s^{(1)}(Kr)$ changes slowly with increasing s and thus the change of amplitude of each term corresponding to a change in index s is essentially proportional to $|\sin \delta_s(Ka) \cos s\phi|$. The term $\cos s\phi$ is one at most and from the tables referred to above,[22] it is seen that $\sin \delta_s(Ka)$ tends to zero with increasing s, (for s greater than a certain integer). Thus by reference to these tables it is possible to pick out the greatest integer s for which any significant contribution will be made to the summation for the scattered field. This maximum integer may then be used as a guide in deciding upon the number of equations to be solved in the two-cylinder problem. Thus for $Ka = 3.0$ $(2a/\lambda \sim 1)$

s =	0	1	2	3
$\vert \sin \delta_s(Ka) \vert =$	0.5680	0.7222	0.9496	0.4977

4	5	6	7
0.1426	0.02251	0.002094	0.000175

and s = 6 is the largest index giving an appreciable term in the field summation. Hence in the two-cylinder problem at least 6 modes must be solved for corresponding to t = 0, ± 1, ± 2, ± 3, . . . ± 6. There is an enormous amount of labor* involved in solving such a system of equations with complex coefficients; however, for a spacing of one wavelength between centers such a system of equations has been solved exactly for the case Ka = 1.253, and approximately for Ka = 2.0 and 2.5, for t ranging between values determined by the above procedure.

Methods of solving such systems of equations on a desk calculator are well known, and the relative merits of one exact method of solution and one method of approximate solution are discussed briefly in Appendix B. Suffice it to say here that except for Ka < 1.30 the labor required to solve such a system on a desk calculator limits somewhat the usefulness of the theory. That the solution of a "block" out of the matrix equation yields results in excellent agreement with measurements may be readily appreciated by a glance at Fig. 9. Here equation(15) has been used to calculate the scattered field.

A Further Approximation

In view of the computational difficulties encountered in solving a large number of linear algebraic equations with complex coefficients it is desirable to have a simple approximation to the solutions for the unknowns $a_{1,s}$, so that some of the major characteristics of the scattering by two cylinders may be more readily seen. The simplest and only approximation that will be

\- - - - - - -

* See Appendix B.

discussed is suggested by the fact that the diagonal elements in the K matrix increase without bound with increasing t, and at the same time the off-diagonal terms tend to zero. Hence it would seem reasonable to neglect completely all off-diagonal terms in calculating the $a_{1,s}$. A glance at Fig. 6 should make it apparent that in general it will be difficult to determine in advance the success of this assumption in predicting measurable quantities from the relative amplitudes of the various elements (diagonal and off-diagonal) in the K matrix because any measurable quantities such as the surface-current distribution or scattered field are derived by complicated summations involving the unknowns $a_{1,s}$. At this point, experiment will prove to be a powerful companion tool to the theory and further discussion along these lines will be found in Section 9. Following then, is a presentation of the analytical results derivable from the use of only the diagonal elements in the K matrix.

From equation (17) the diagonal elements in a K matrix of any order are obtained by using the symmetry relationship previously derived, namely

$$a_{-1,t} = a_{1,-t} \quad ;$$

and selecting only the coefficients of these unknowns from the equation corresponding to each value of t (taking t = s for convenience of notation). Thus for a line source

$$a_{1,s} = \frac{4i(-)^s H_s^{(1)}(K\sqrt{r_o^2 + b^2})e^{-is\theta_1}}{H_s^{(1)}(Ka) + J_s(Ka)H_{2s}^{(1)}(2Kb)} \tag{19}$$

The value for the 'scattering coefficients' $a_{1,s}$ may be substituted into equation (7) to give the following approximate expression for the scattered field.

$\psi^{scatt}(R,\phi) =$

$$-\sum_{n=\pm 1}\sum_{s=-\infty}^{\infty}(-)^s \frac{J_s(Ka)H_s^{(1)}(K\sqrt{r_o^2+b^2})H_s^{(1)}(KR_n)e^{is(\phi_n-\theta_1)}}{H_s^{(1)}(Ka) + J_s(Ka)H_{2s}^{(1)}(2Kb)} \tag{20}$$

In the limit, as Kb and $Kr_o \longrightarrow \infty$, this expression (except for an unimportant constant) is identical with Seitz's[16] expression for the field scattered by an isolated cylinder (provided the summation over the cylinders is extended to one cylinder only). Also as $Kb \longrightarrow \infty$ each term in the series becomes that predicted by the independent scattering hypothesis. For small cylinders (i.e., small Ka) the Bessel and Hankel functions involving Ka may be approximated by their power series representations to give the following result for the scattered field, (in the case that $b \gg a$).

$\psi^{scatt}(R,\phi) \sim$

$$\frac{-\sum_{n}\sum_{s=-\infty}^{\infty}(-1)^s\left(\frac{Ka}{2}\right)^s \frac{1}{s!}\; H_s^{(1)}(K\sqrt{r_o^2+b^2})H_s^{(1)}(KR_n)e^{is(\phi_n-\theta_1)}}{\left\{\begin{matrix} -\frac{2i}{\pi}\ln\frac{2i}{\gamma Ka} & s = 0 \\ -\frac{(s-1)!}{\pi}\left(\frac{2}{Ka}\right)^s & s \neq 0 \end{matrix}\right.}$$

From this result it is easily seen that for small cylinders the major contribution to the scattered field comes from the mode with $s = 0$. If KR_n, $Kr_o \gg 1$ the amplitude of the functions $H_s^{(1)}(K\sqrt{r_o^2+b^2})$ and $H_s^{(1)}(KR_n)$ is approximately constant for different s; hence the relative amplitudes of the zeroth and first mode in the scattered field are

$$\left|\frac{1}{2\log_\varepsilon\left(\frac{2i}{\gamma Ka}\right)}\right| \text{ and } \left(\frac{Ka}{2}\right)^2$$

where $\gamma = 1.7811 \ldots$

The following table compares these quantities for K = 0.25 and 0.50

Ka	Zeroth Order $\frac{1}{2\log_\varepsilon \frac{2i}{\gamma Ka}}$	1st Order $(\frac{Ka}{2})^2$
0.25	0.230	0.0156
0.50	0.238	0.0625

Thus for $Ka < 0.25$ only the zeroth mode need be considered, and for Ka in the range 0.25 to 0.50 contributions from the next mode begin to be appreciable. Thus (by neglecting coupling) we have a simple criterion for defining the small cylinder. In Fig. 9 the result of calculating the field at a fixed point from the zeroth mode, or uniform surface-current distribution (coupling taken into account) is plotted as a function of the radius a, for a fixed spacing of one wavelength between centers.

The diminishing effects of coupling on the coefficients $J_s(Ka)a_{1,s}$ in (20) occurring in the summation of equation (19) as s is increased may be seen in the following way. Assuming that the source and point of observation are both a large distance from the cylinders, the contribution of each mode in equation (20) is proportional to

$$\alpha_s(Ka,Kb) = \frac{J_s(Ka)}{H_s^{(1)}(Ka) + J_s(Ka)H_{2s}^{(1)}(2Kb)} \qquad (21)$$

As s increases, and for Ka, $Kb \gg 1$ the approximations for the Bessel and Hankel functions leading to equation (8) give for (21) the following asymptotic form:

$$\alpha_s(a,b) \sim \frac{1}{(\frac{2t}{Ka})^{2t} + \frac{1}{\sqrt{2\pi t}}(\frac{2t}{Kb})^{2t}}$$

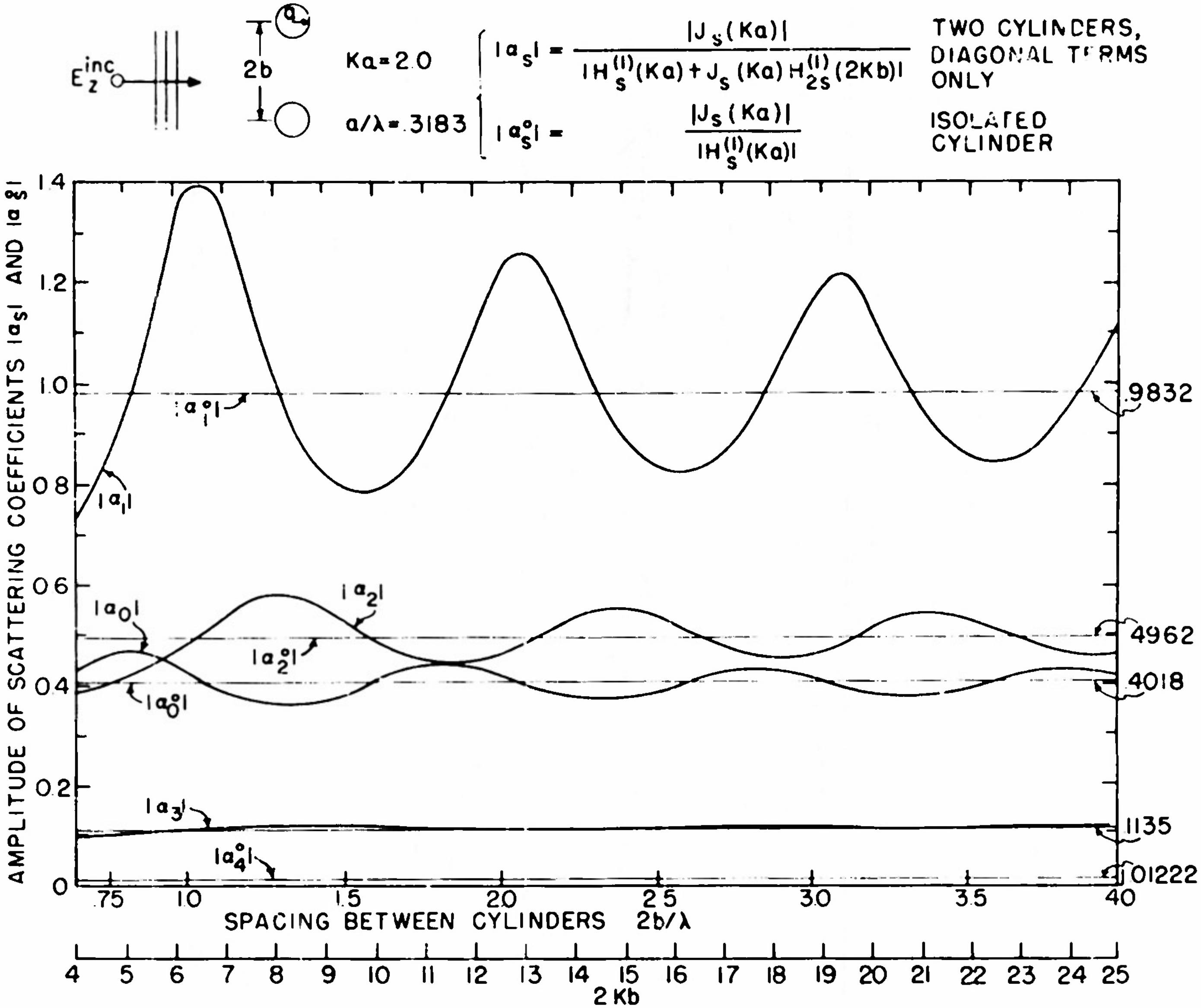

FIG. 7 SCATTERING COEFFICIENT $|a_s|$ AND $|a_s^o|$ FOR TWO COUPLED CYLINDERS (DIAGONAL TERMS ONLY) AND AN ISOLATED CYLINDER AS A FUNCTION OF SPACING BETWEEN CENTERS FOR Ka = 2.0 AND NORMAL INCIDENCE

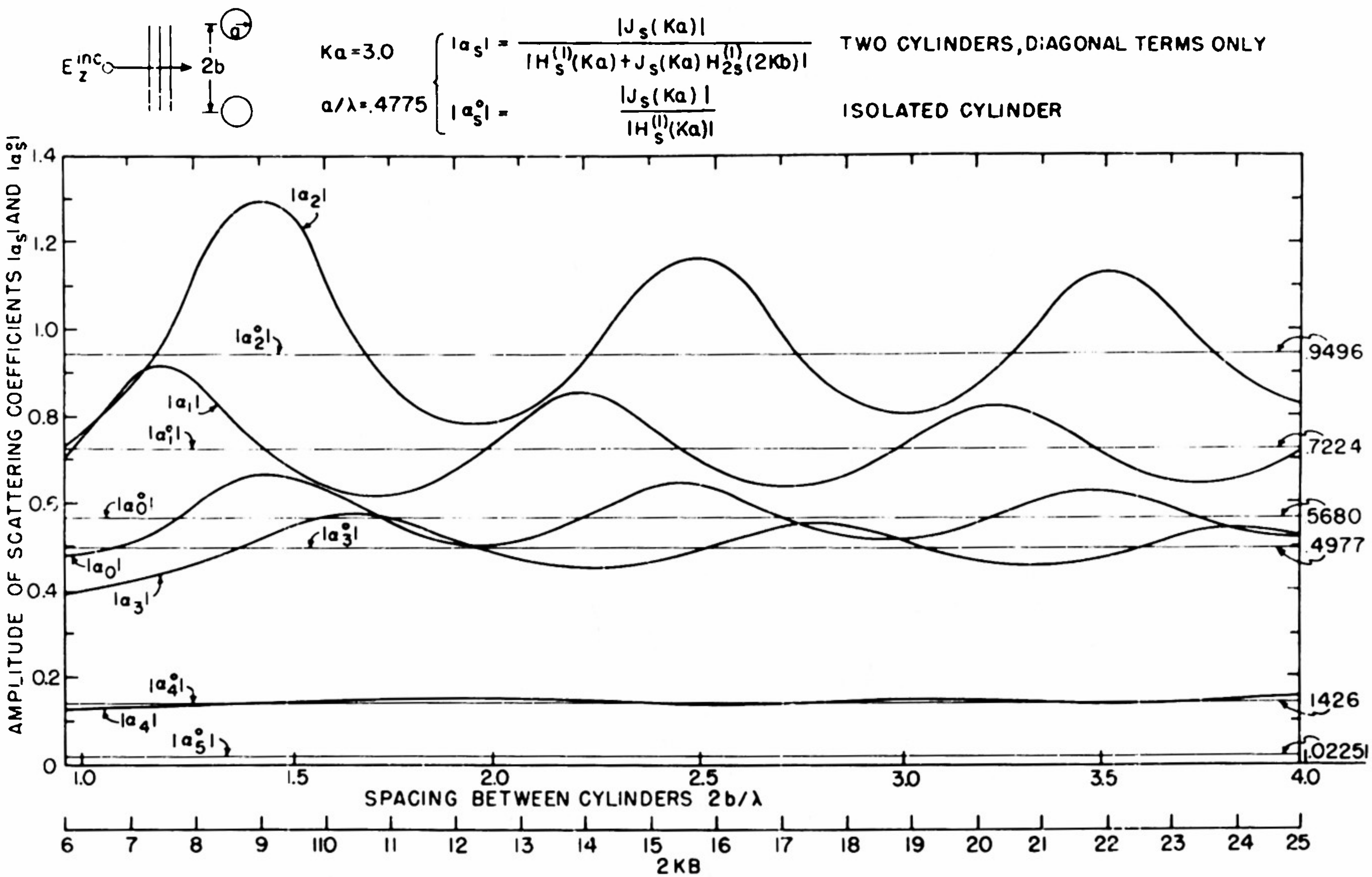

FIG. 8 SCATTERING COEFFICIENTS $|a_s|$ AND $|a_s^o|$ FOR TWO COUPLED CYLINDERS (DIAGONAL TERMS ONLY) AND AN ISOLATED CYLINDER AS A FUNCTION OF SPACING BETWEEN CENTERS FOR Ka = 3.0 AND NORMAL INCIDENCE

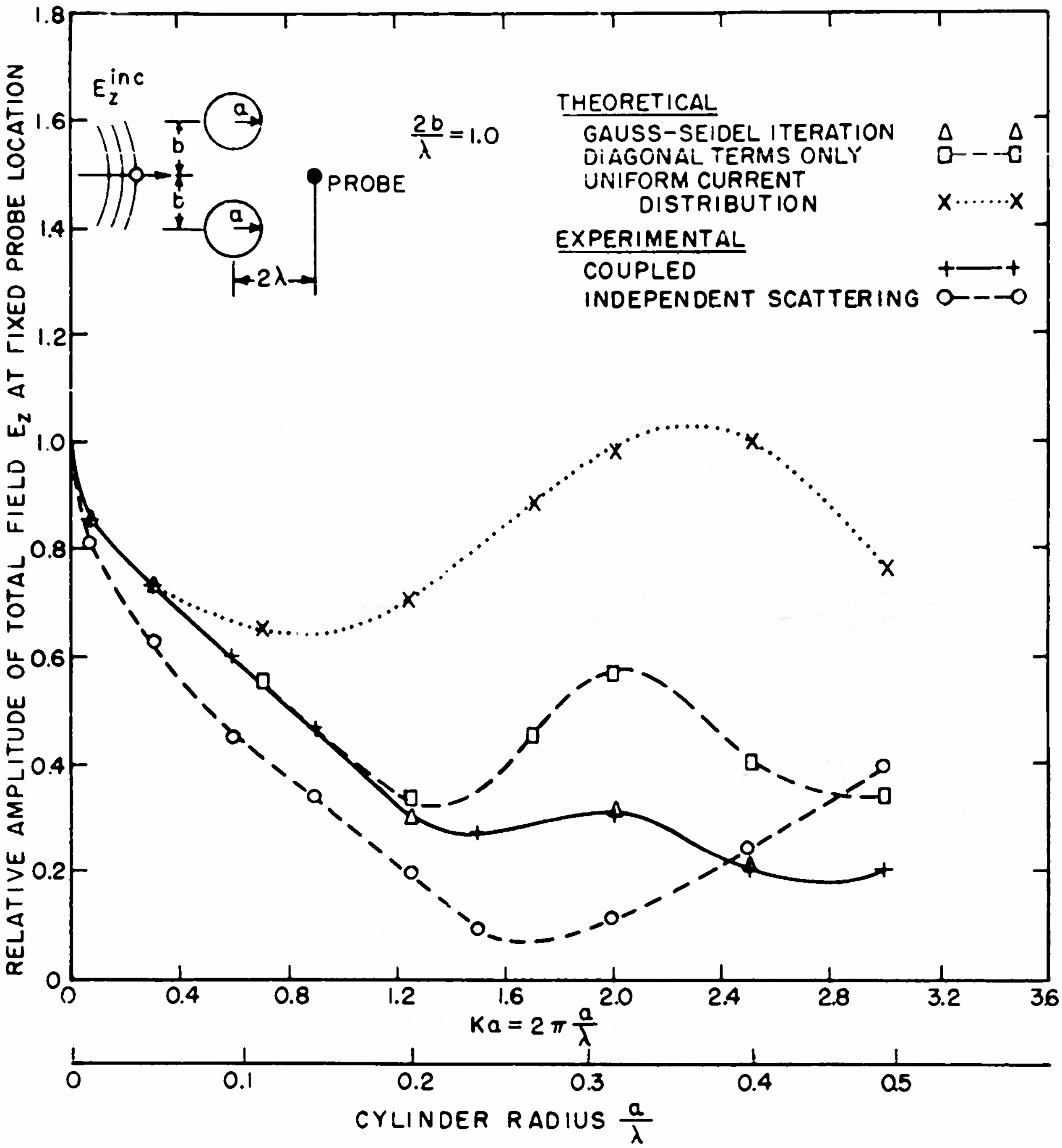

FIG. 9 AMPLITUDE OF FIELD SCATTERED BY TWO IDENTICAL CYLINDERS, FOR FIXED PROBE LOCATION AND SPACING $\frac{2b}{\lambda} = 1.0$ AS A FUNCTION OF RADIUS OF CYLINDERS (LINE SOURCE)

where the right-hand term in the denominator contains the coupling effect. From this last expression it is apparent, since b is always greater than or equal to a, that the two cylinders influence each other to a decreasing extent as the mode index s increases. This behavior is most strikingly demonstrated by the graphical plots of $|\alpha_s|$ as a function of spacing for K = 2.0 and 3.0 shown in Figs. 7 and 8. Here the complete expression for α_s given in (21) was used in the computations. In addition, $|\alpha_s^o|$, the corresponding quantity for an isolated cylinder, is plotted along with $|\alpha_s|$ for comparison. It is seen that the coefficient α_s approaches the corresponding α_s^o for the isolated cylinder in an oscillating manner and for the higher modes (for example, s = 3,4,5 and Ka = 3.0 in Fig. 8) the relative amplitude of these oscillations is small. In addition, these oscillations damp rather slowly with increasing separation between the cylinders, indicating qualitatively at least that mutual effects tend to diminish rather slowly with increasing separation, although the complexity of the expression (20) relating the coefficients α_s to the scattered field makes it difficult to predict solely on the basis of a graphical picture of the α_s how the total field will depend on spacing and radius.

To compare the predictions of the 'diagonal' approximation to measurable field quantities equation (20) has been used to calculate the scattered field. For large separation between source and cylinders the following representation* is used for the Hankel function $H_s^{(1)}(K\sqrt{r^2 + b^2})$ in equation (20)

$$H_s^{(1)}(Ku) \sim \sqrt{\frac{2}{\pi Ku}}\, e^{i(Ku - \frac{\pi s}{2} - \frac{\pi}{4})}\left[S_s^{(1)}(Ku) + O\left(\frac{1}{Ku}\right)^p\right] \qquad (22)$$

where $u = \sqrt{r_o^2 + b^2}$ and

$$S_s^{(1)}(Ku) = \sum_{m=0}^{p-1} \frac{(-1)^m\,\Gamma(s+m+\frac{1}{2})}{(2iKu)^m\; m!\;\Gamma(s-m+\frac{1}{2})}$$

* See General References, Watson's "Bessel Functions," p. 198.

Since $Kr_o \gg s$ and $K = \frac{2\pi}{\lambda}$, equation (20) for the scattered field reduces to

$$\psi^{scatt} = -\frac{e^{-i\pi/4}}{\pi}\sqrt{\frac{\lambda}{\sqrt{r_o^2+b^2}}}\, e^{iK\sqrt{r_o^2+b^2}}$$

$$\sum_n \sum_s e^{\frac{\pi i s}{2}} \alpha_s(Ka,Kb) S_s^{(1)}(Ka,Kb)(K\sqrt{r_o^2+b^2}) H_s^{(1)}(KR_n) e^{is(\phi_n-\theta_1)}$$

The incident field at $x = x$, $y = 0$ is

$$\psi^{inc}(x,0) = \frac{e^{-i\pi/4}}{\pi}\sqrt{\frac{\lambda}{r_o+x}}\, e^{iK(r_o+x)} S_o^{(1)}(K(r_o+x))$$

and for $K(r_o+x) \gg 1$, $S_o^{(1)} \sim 1$. The total field can now be calculated using the definition

$$\psi^{tot} = \psi^{inc} + \psi^{scatt} .$$

Dividing this expression by the incident field at the reference point $x = x$, $y = 0$ gives for the normalized field

$$\psi_{norm}^{tot}(x,y) = E_z = 1 - \sqrt{\frac{r_o+x}{\sqrt{r^2+b^2}}}\, e^{iK\sqrt{r_o^2+b^2}-iK(r_o+x)} \times$$

$$\sum_{n\pm1} \sum_{s=-\infty}^{\infty} e^{\frac{\pi i s}{2}} \alpha_s(Ka,Kb) S_s^{(1)}(K\sqrt{r^2+b^2}) H_s^{(1)}(KR_n) e^{is(\phi_n-\theta_n)} \qquad (23)$$

This formula has been used in calculating the theoretical results labeled, diagonal terms only, in Fig. 6 of this section and Figs. 16, 19, through 21 of Section 5. In these results Kb has been fixed and Ka allowed to vary (from 0.0783 to 3.0) and vice versa, (2b varying from 1 to 8 wavelengths).

Effect of Line-Source Excitation.

The use of a line source for the primary excitation shows up in two places in the general theoretical formulation exemplified in the matrix equation of Fig. 6. Firstly, as an amplitude and phase factor in the term $H_t^{(1)}(K\sqrt{r_o^2+b^2})$ on the right-hand side of the matrix equation. The general behavior of this term may be studied through the representation of the Hankel function stated in (22). In addition the general recurrence formula*

$$H_{s+1}^{(1)}(z) = \frac{2s}{z} H_s^{(1)}(z) - H_{s-1}(z)$$

may be used to give the relation

$$S_{s+1}^{(1)}(z) = \frac{2s}{z}\, i\, S_s^{(1)}(z) + S_{s-1}^{(1)}(z) \qquad (24)$$

valid for $z \gg 1$. In particular $S_o^{(1)}(z)$ and $S_1^{(1)}(z) \sim 1$.

The use of these relations in (22) shows that for small t

$$H_t^{(1)}(K\sqrt{r_o^2+b^2}) \sim \sqrt{\frac{2}{\pi K\sqrt{r_o^2+b^2}}}\; e^{i(K\sqrt{r_o^2+b^2} - \pi s/2 - \pi/4)}$$

This expression contains the familiar cylindrical wave amplitude factor $1/\sqrt{[K\sqrt{r_o^2+b^2})]}$, which reduces the amplitude of excitation on each cylinder as the spacing increases. In addition there is a phase retardation factor $e^{iK\sqrt{r_o^2+b^2}}$. Both of these factors are more or less independent of the order t. As t becomes large the factor $2s/[\sqrt{K\sqrt{r^2+b^2}}]$, appearing in the expression (24) for $S_{s+1}^{(1)}(K\sqrt{r_o^2+b^2})$ increases in importance. However the occurrence of this increasing factor causes little effect on the field because it is multiplied by $\alpha_s(Ka,Kb)$ in the summation for the scattered field and thus the product $\alpha_s(Ka,Kb)S_s^{(1)}(K\sqrt{r_o^2+b^2}$ tends to zero with increasing s. In addition to the factors on the right of the matrix equation which are approximately independent of order there are two phase factors which depend linearly on the order. One comes from $H_t^{(1)}(K\sqrt{r_o^2+b^2})$, and the other is $e^{\pm it\theta_1}$. Using the asymptotic expansion for the Hankel function they may be combined into the one factor

* - - - - - -

*See General Bibliography, Watson's "Bessel Functions," p. 74.

For Θ_1 small, that is, the separation between cylinders small compared to their distance from the source, the contribution of the factor $e^{\pm it(\frac{\pi}{2} - \theta_1)}$ of the factor $e^{\pm it\,\theta_1}$ is negligible for small t. The factor $e^{\pm it\pi/2}$ is the same phase factor that occur for plane wave excitation and hence is of little interest here. The effect of all these excitation factors on the total field may best be summarized by reference to equation (23). For convenience take the point of observation to lie along the direction of incidence so that $\phi_1 = -\phi_{-1}$, and of course $\Theta_1 = -\Theta_{-1}$. Thus (23) simplifies to

$$E_z = 1 - 2\sqrt{\frac{r_o+x}{\sqrt{r^2+b^2}}}\; e^{iK\sqrt{r_o^2+b^2}-iK(r_o+x)}\,.$$

$$\sum_{s=0}^{\infty} \varepsilon_s e^{\frac{\pi i s}{2}} \alpha_s(Ka,Kb)S_s^{(1)}(K\sqrt{r_o^2+b^2}) \times$$

$$H_s^{(1)}(KR_1)\cos s(\phi_1-\theta_1)\,.$$

In the far zone, $H_s^{(1)}(KR_1) \sim \frac{e^{-i\pi/4}}{\pi}\sqrt{\frac{\lambda}{R_1}}\, e^{iKR_1 - i\pi s/2}S_s^{(1)}(KR_1)$ and $\phi_1 \approx 0$.

Therefore

$$E_z\Big|_{\substack{\text{cylindrical}\\ \text{wave}}} \sim 1 - \frac{2e^{-i\pi/4}}{\pi}\sqrt{\frac{r_o+x}{\sqrt{r_o^2+b^2}}}\; e^{iK\sqrt{r_o^2+b^2} - iK(r_o+x)+iKR_1}\sqrt{\frac{\lambda}{R_1}} \times$$

$$\sum_{s=0}^{\infty} \varepsilon_s \alpha_s(Ka,Kb)S_s^{(1)}(K\sqrt{r_o^2+b^2})S_s^{(1)}(KR_1)\cos s\theta_1 \qquad (25)$$

The corresponding expression for plane-wave excitation is obtained by allowing b to approach infinity, thus

$$E_z\Big|_{\substack{\text{plane}\\\text{wave}}} \sim 1 - \frac{2e^{-i\pi/4}}{\pi}\sqrt{\frac{\lambda}{R_1}}\; e^{-iKx + iKR_1} \sum_{s=0}^{\infty} \varepsilon_s a_s(Ka,Kb)S_s^{(1)}(KR_1)$$

Comparison of these two expressions shows that for the point of observation on the side of the cylinders away from the source the scattered wave in the line source case is modified by the amplitude factors

$$\sqrt{\frac{r_o + x}{\sqrt{r_o^2+b^2}}} \quad \text{and} \quad S_s^{(1)}(K\sqrt{r_o^2+b^2})\cos s\theta_1 \quad .$$

For θ_1 (i.e. $r_o >> b$) the only significant difference in amplitude for cylinders of moderate diameters is due to the factors $\sqrt{\frac{r_o + x}{\sqrt{r_o^2 + b^2}}}$, which for the cases computed and plotted graphically in this chapter and the next, results at most in about 3 per cent increase in amplitude of the (relative) scattered field above the corresponding amplitude for the plane-wave case. Expanding $K\sqrt{r_o^2+b^2}$ in a binomial series for $b^2 << r_o^2$ and keeping only the first two terms gives

$$e^{iK\sqrt{r_o^2+b^2} - iKr_o} \sim e^{iKb^2/2r_o} + \ldots .$$

Hence for $b^2 << r_o$ there is only a slight retardation in the phase of the scattered field for the line source compared to the same field for plane-wave excitation. However, for b as large as 4 wavelengths and r_o=37.7 wavelengths (corresponding to an actual experimental condition) the phase retardation is as large as 88.2 degrees and must be taken into account in the computation.

In the experimental measurements designed to check the results of the theory, the separation of source and cylinders has been kept constant at 37.7 wavelengths.

5. Measurements of the Field Scattered by Two Identical Conducting Cylinders (For Normal Incidence)

The parallel-plate region and associated field-probing equipment described in Technical Report 153 have been used in a series of measurements of the field scattered by two identical highly conducting cylinders with a uniform line source for the primary excitation (at normal incidence) as sketched in Fig. 5.

These measurements are designed as a check on the validity of the approximations made in the theory developed in the preceding section; and to compare the predictions of the independent scattering hypothesis with the fields actually measured.

Changes in Equipment.

No changes have been made in the field-probing equipment as described in Technical Report No. 153. However, two minor changes were made in the arrangement of the source; and a set of retractable positioning pins (which also serve as the smaller diameter scattering cylinders) and a moveable spacing bar were added to the probe-panel assembly.

In order to obtain a smoother amplitude distribution of the incident field along the line of probe travel the flanges on the waveguide horn-radiator were removed. This largely eliminated fluctuation in the incident field along the line of probe travel due to diffraction effects cuased by the finite aperture of the horn. The previous difficulty with the use of an unflanged guide as a radiator was the fluctuation in the probe signal strength whenever the parallel plates were opened and closed again. This fluctuation has been removed by coating the top and bottom surfaces of the guide with a very slow drying silver paint which tends to maintain uniformly good electrical contact between the waveguide and parallel plates whenever the plates are opened and closed again. The absorbing wedges at the edge of the plates near the waveguide have been kept at least 2 wavelengths from the open end of the guide, so that small changes in their position with opening and closing of the plates now causes negligible changes in the incident field measured at the probe. This radiating system has a measured phase center at approximately 39.7 wavelengths from the mid-point of the probe travel at the operating wavelength of 3.185 cm. In addition the 3-cm oscillator has been moved much closer to the open end of the radiating guide. This results in a shorter electrical transmission path from the oscillator to the phase reference line and field probe, thereby improving considerably the reproducibility of phase measurements.

To permit quick and accurate positioning of the scattering cylinders in the parallel-plate region a retractable set of 1/8-inch diameter Dural pins has been added to the probe panel assembly. These pins are spaced along a line parallel to the probe travel line and two wavelengths (wavelength = 3.185 cm.) from it on the side towards the source. They protrude into the parallel-plate region as shown in Fig. 10 and allow the scattering cylinders and/or spacing bar with a corresponding 1/8-inch diameter hole to be fitted over them. The pins are spaced 1/2 wavelength between centers with the first pin located on the line joining the phase center of the horn to the mid-position of the probe travel. Each 1/8-inch diameter pin is drilled along its axis to take a 1/32-inch diameter coin silver wire, which may also be pushed up into the parallel-plate region. The 1/32-inch diameter wire and 1/8-inch diameter pin thus serve as scattering cylinders with $Ka = 0.0783$ and 0.313 respectively. The probe panel assembly complete with the positioning pins is shown in Fig. 11.

To permit cylinder spacings at other than 1/2 wavelength steps a series of spacing bars were constructed. They consist simply of a 10-inch long rectangular bar of Dural, 1/2 x 3/8 inch in cross section, with a brass sleeve which fits over any of the 1/8-inch diameter positioning pins. At convenient positions along its length 1/8-inch diameter holes may be drilled and fitted with easily removeable brass pins. The brass pins are used to locate the scattering cylinders on the spacing bar and the whole assembly is then inserted into the parallel plate region, the sleeve being inserted over one of the positioning pins. Figure 12 shows a sketch of a particular spacing bar used in this way. After the scattering cylinders have been located the spacing bar is removed and the positioning pin pushed down till its end is flush with the surface of the lower plate. The upper plate may now be lowered into position on top of the cylinders.

Scattering Cylinders and Experimental Technique

Each cylinder used was made from brass turned to the correct diameter and 0.500 + 0.005 inches thick. A 1/8-inch diameter hole was drilled through the center to allow easy and accurate location of the cylinder on the system of positioning pins just described. To insure good electrical contact with the parallel plates, the top and bottom surfaces of the cylinder were lightly coated with the slow drying silver paint.

The results to be presented showing the total electric field as a superposition of the field scattered independently by each cylinder are determined in accordance with the independent scattering hypothesis. Thus, if $E_z^{inc}(\vec{r})$ is the incident electric field at a point $\vec{r}$ and $E_z^{tot}(\vec{r})$ is the total electric field with cylinder 1 in place, then $E^{scatt}(\vec{r}) = E_{z_1}^{tot}(\vec{r}) - E_z^{inc}(\vec{r})$. Similarly if cylinder 1 is removed and cylinder -1 is put in place

$$E_{z_{-1}}^{scatt}(\vec{r}) = E_{z_{-1}}^{tot}(\vec{r}) - E_z^{inc}(\vec{r}) \quad .$$

According to the independent scattering hypothesis the total field with both cylinders in place is given by

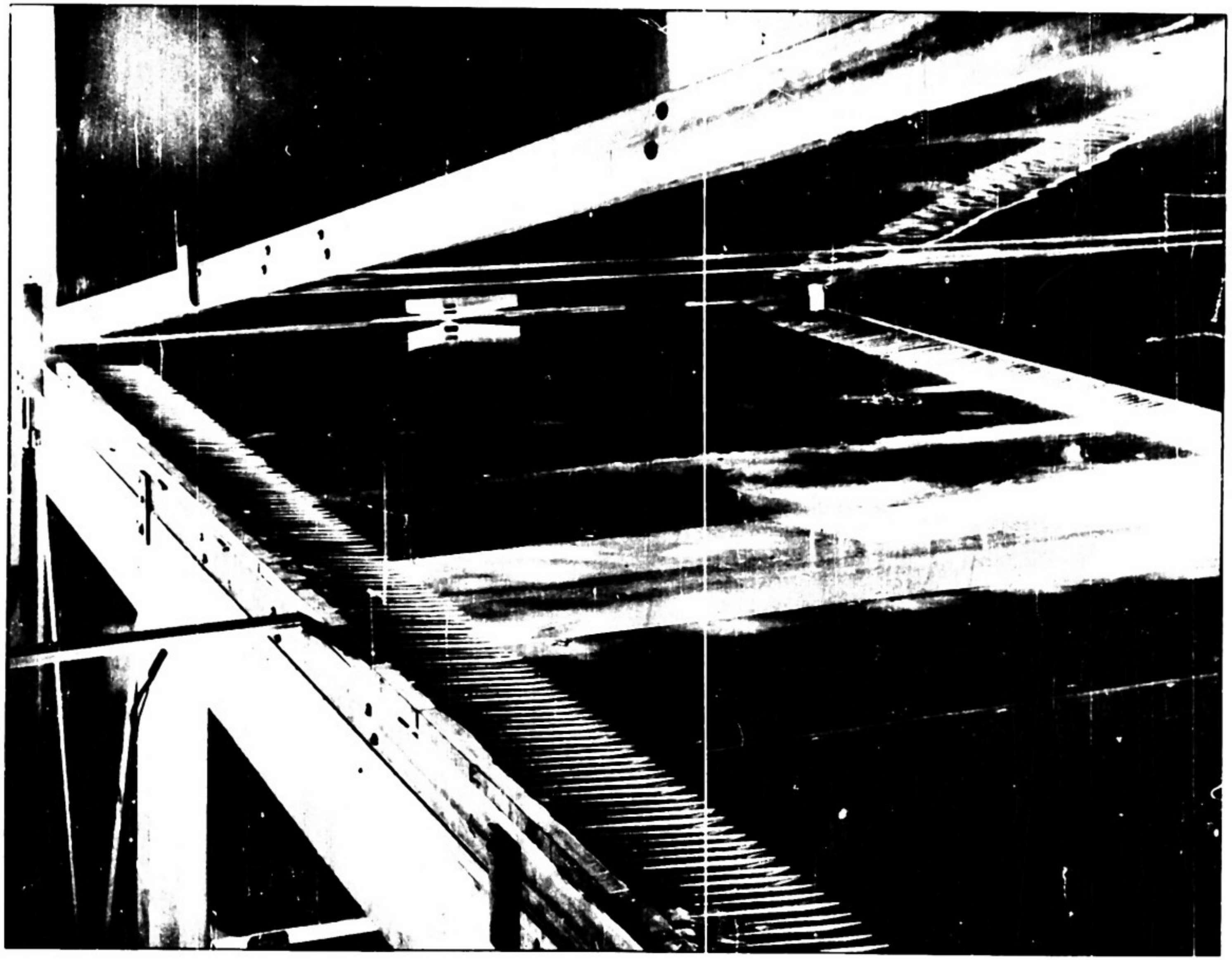

FIG. 10 PARALLEL PLATES OPENED TO SHOW RETRACTABLE PINS USED TO POSITION SCATTERING CYLINDERS

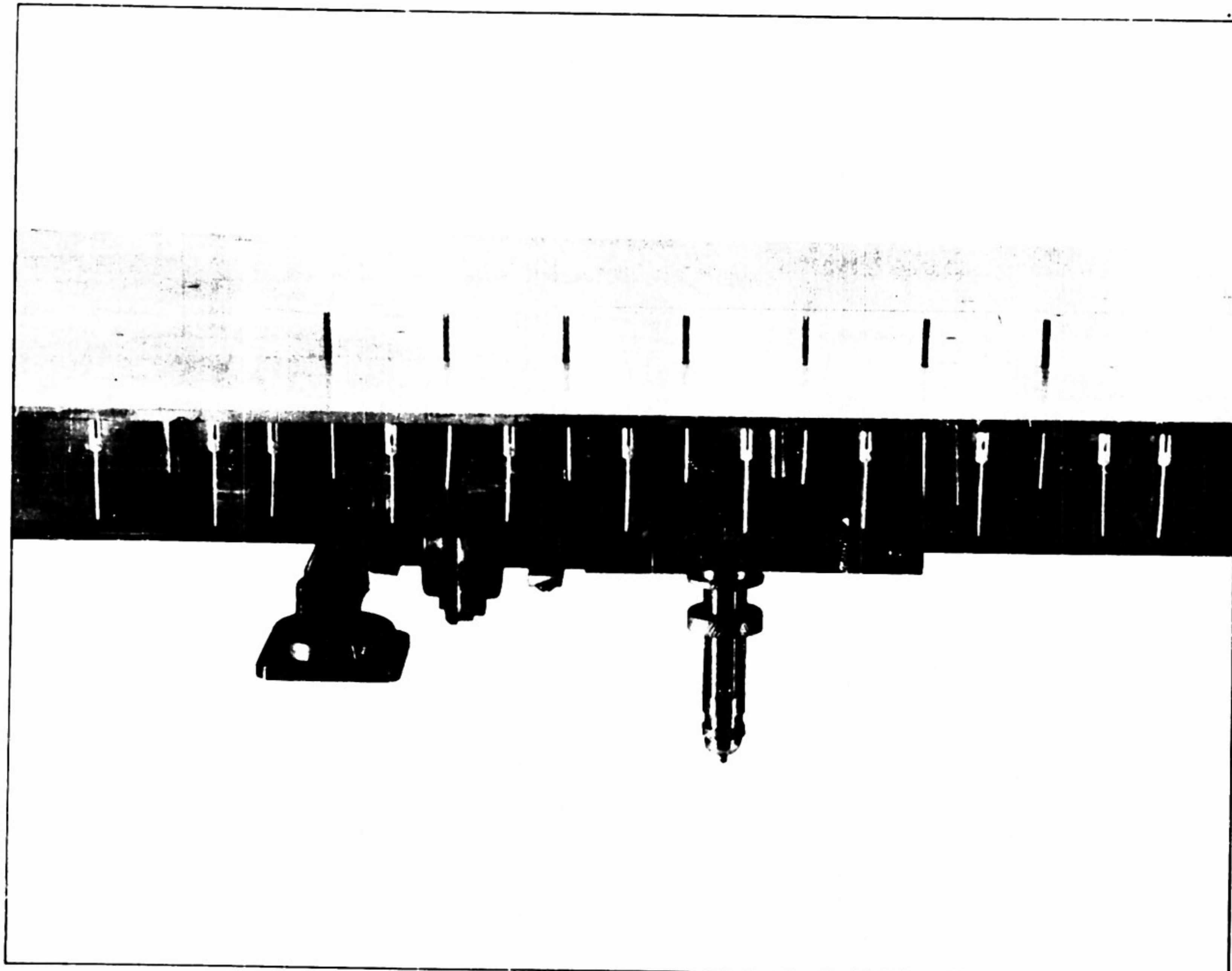

FIG. 11 PANEL CARRYING PROBE ASSEMBLY, REMOVED TO SHOW RETRACTABLE PINS USED TO POSITION CYLINDERS IN PARALLEL PLATE REGION

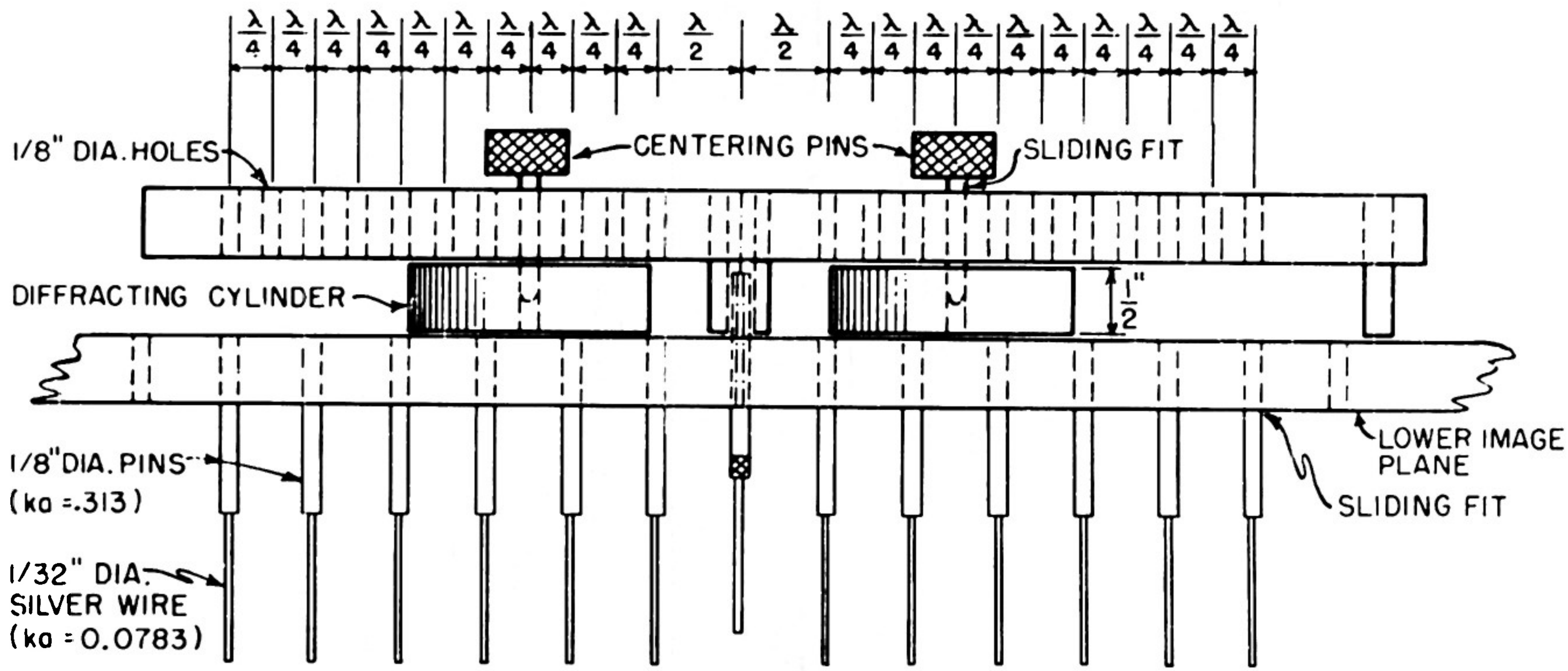

FIG. 12 CROSS SECTION OF RETRACTABLE PINS AND ADDITIONAL SPACING BAR FOR LOCATING DIFFRACTING CYLINDERS IN PARALLEL PLATE REGION

$$E_z^{tot}(\vec{r}) = E_z^{inc}(\vec{r}) + E_{z_1}{}^{scatt} + E_{z_{-1}}{}^{scatt}$$

$$= E_{z_1}^{tot}(\vec{r}) + E_{z_{-1}}^{tot}(\vec{r}) - E_z^{inc}(\vec{r})$$

The results labeled "independent scattering' in the following graphs were calculated from the formula immediately above, following a measurement of the amplitude and phase of the incident and total fields as outlined in the preceding procedure.

Measurements.

Amplitude measurements are reproducible to closer than 2 percent in all cases and in some cases where the signal is relatively large, the results may be reproduced to within 1 per cent as in Figs. 15 and 16 and Fig. 18 through Fig. 22 where the probe position was kept fixed. Phase measurements are uncertain to within about ± 2 degrees and reproducible to about the same degree.

The measurements made may be separated into two classes. Those where the cylinder spacing and radius are fixed and the probe moves along the line parallel to and 2 wavelengths from (on the side away from the source) the line joining the centers of the cylinders, and those where the probe is fixed and the cylinder spacing and radius are allowed to change. The first type of measurement gives a curve of the actual diffraction field in the near zone and serves as an overall comparison between theory and experiment. Figures 13 - 16 show the relative amplitude of the total field as a result of such measurements with cylinders one wavelength between centers, and radii corresponding to Ka = 0.0783, 0.313, 1.253 and 2.000. A spacing of one wavelength was chosen to permit sizable coupling between cylinders about a wavelength in diameter and still have the radius small enough to require the solution of the matrix equation of Fig. 6 for only half a dozen mode coefficients. For the two smaller cylinders no graphical results are presented for the independent scattering hypothesis. The reproducibility of phase and amplitude measurements introduces relatively larger uncertainties in the calculation of the independent scattered field for small cylinders because the total field and incident field are more nearly equal than for the larger scatterers which cause greater differences between the incident and scattered fields. In general this first type of measurement requires a relatively large amount of labor for a relatively small amount of information gained about the effects of spacing and radius on coupling between the cylinders. In addition, a large amount of computing is necessarily to calculate such a curve from the theory, since each point on the graph requires summing a series of six or more complex terms.

The second type of measurement affords a simpler experimental study of the importance of spacing and radius on coupling effects and in addition reduces the amount of computing necessary in the theory. For this type of measurement the probe was fixed at a point equidistant from the center of the two cylinders and two wavelengths from the line joining them, on the side away from the source, and the spacing and radius were varied. Figures 17 through 21 show the amplitude of the total field at this point as a function of spacing, for spacings from one to eight wavelengths and radii corresponding to Ka = 0.313, 1.253, 1.50, 2.0 and 3.0. Figures 9 and 22 show the same quantity as a function of radius for Ka ranging from 0.0783 to 3.0 for spacings of 1.0 and 3.024 wavelength.

6. Conclusions

Comparison of Measurements with Theory

Numerical results have been computed from the formulae discussed in Sections 4, 5, and 6, and are plotted along with the appropriate experimental results mentioned in Section 5.

A study of Fig. 9 and Figs. 15 through 22 shows that over

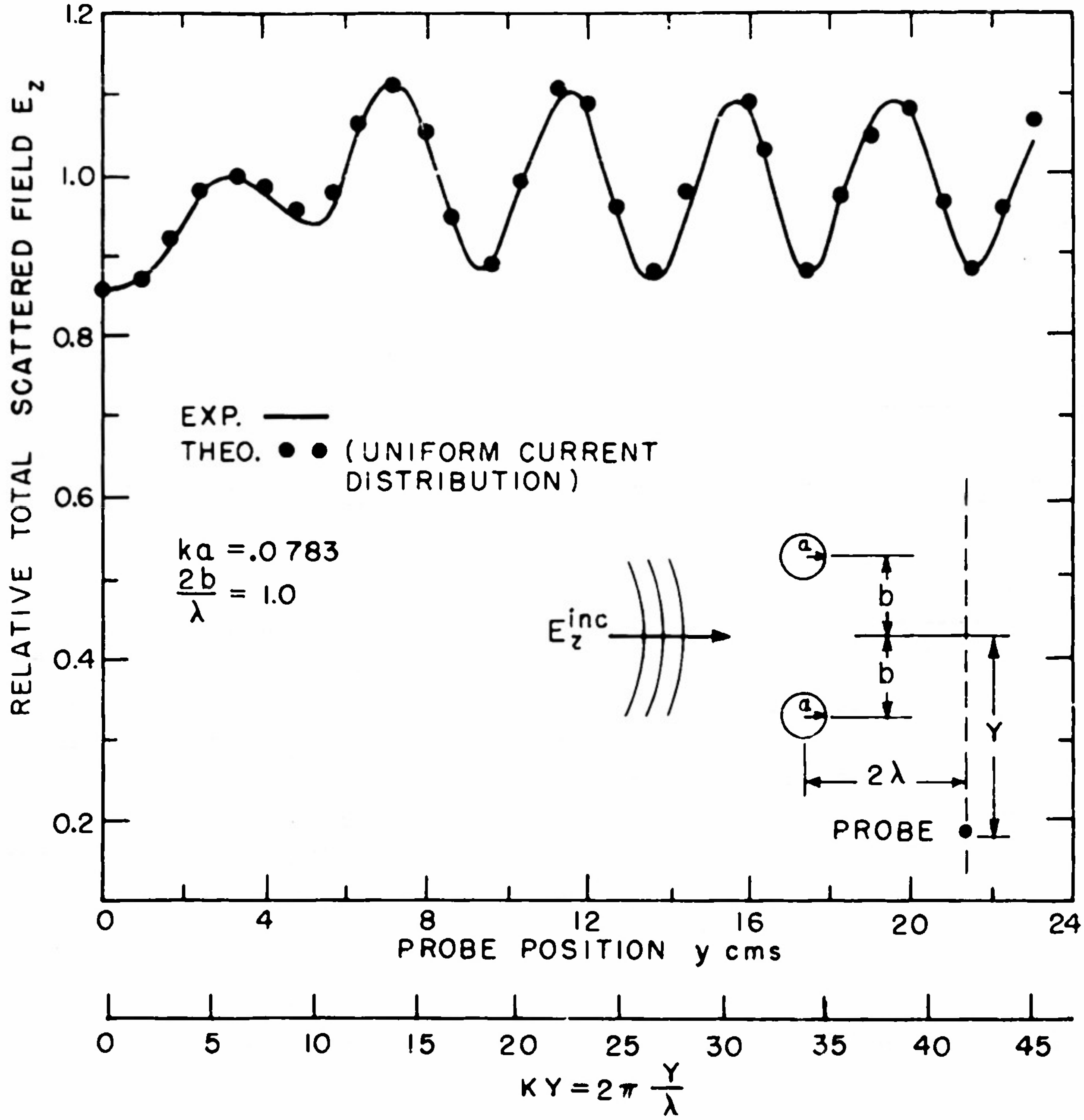

FIG. 13 EXPERIMENTAL AND THEORETICAL RESULTS OF DIFFRACTION BY TWO CYLINDERS AS A FUNCTION OF PROBE POSITION FOR $ka = .0783$ AND SPACED 1.0 WAVELENGTH BETWEEN CENTERS

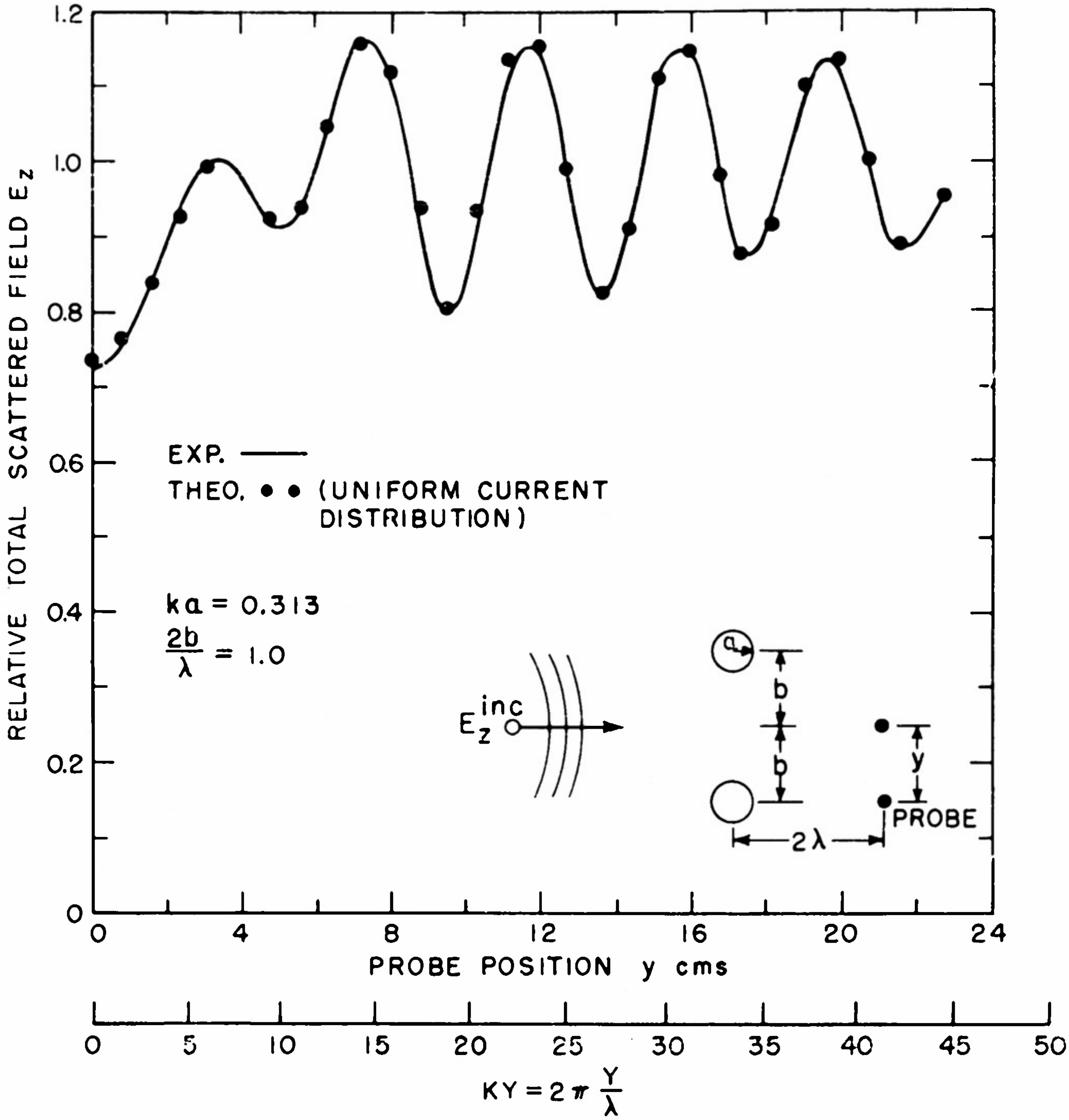

FIG. 14 EXPERIMENTAL AND THEORETICAL RESULTS OF DIFFRACTION BY TWO CYLINDERS AS A FUNCTION OF PROBE POSITION FOR $ka = 0.313$ AND SPACED 1.0 WAVELENGTH BETWEEN CENTERS

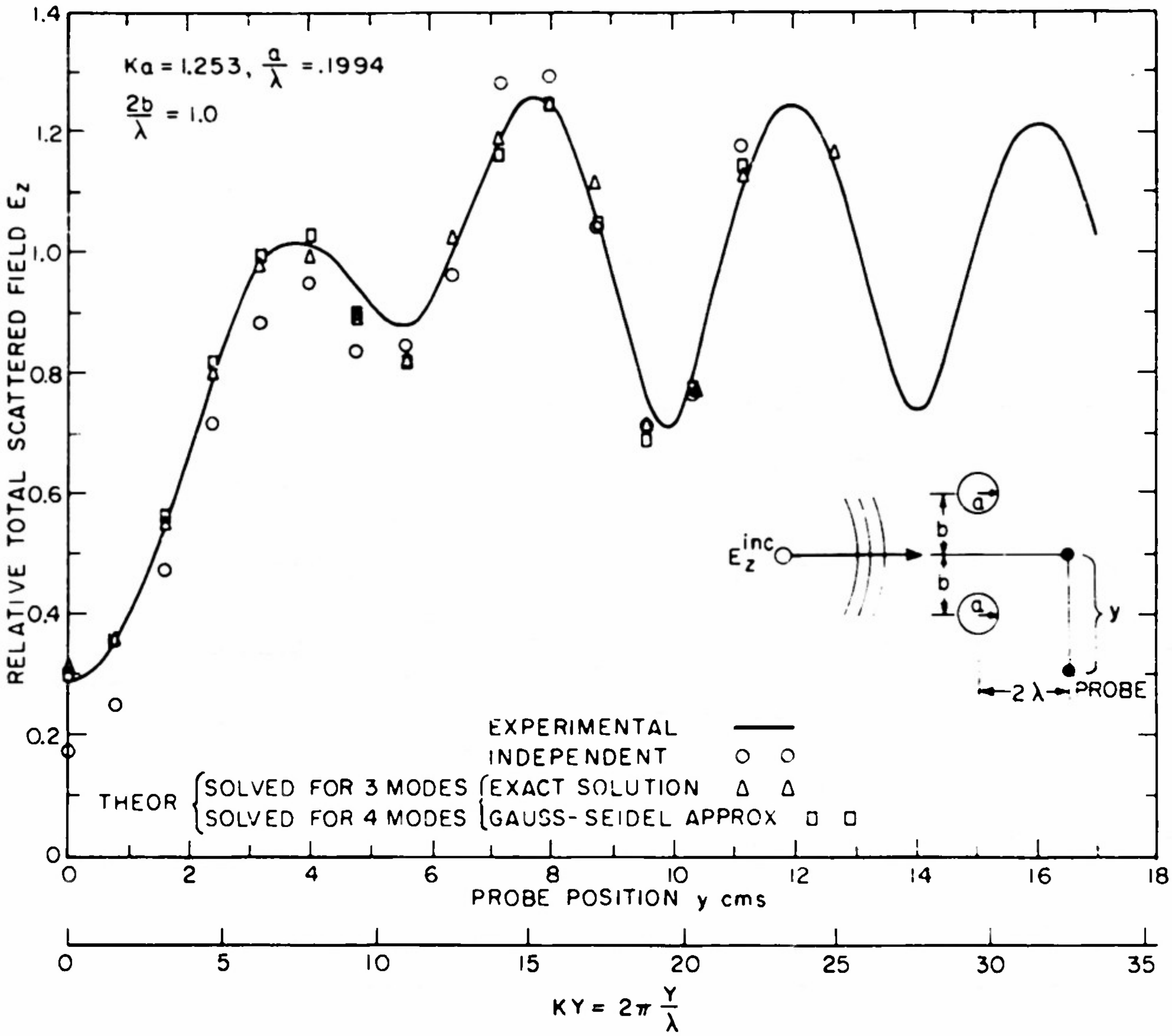

FIG. 15 EXPERIMENTALLY MEASURED DIFFRACTED FIELD FROM TWO CYLINDERS AND COMPARISON WITH VARIOUS THEORETICAL APPROXIMATIONS FOR Ka = 1.253, AS A FUNCTION OF PROBE POSITION

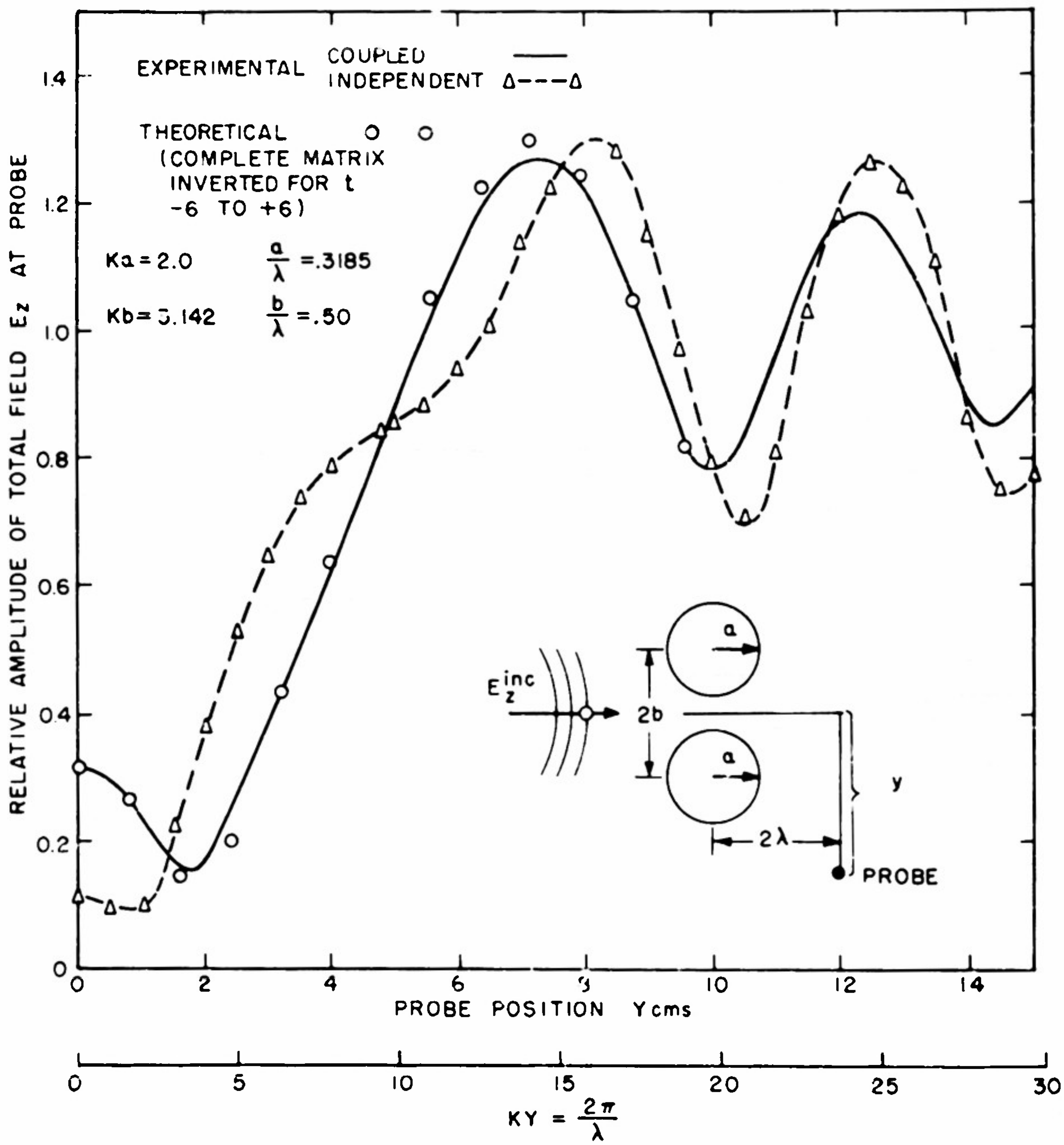

FIG. 16 THEORETICAL AND EXPERIMENTAL DIFFRACTION CURVES FOR SCATTERING FROM TWO IDENTICAL CLOSELY COUPLED CYLINDERS RADIUS $a = .3185\,\lambda$ AND SPACING BETWEEN CENTERS $= 1.0\,\lambda$

a fairly large range of radii and spacings the independent scattering hypothesis may be used to predict large-scale trends in the results, both for diffraction pattern measurements and for those results where the probe was fixed and spacing and radius allowed to vary. Thus for the probe fixed and a constant spacing of 1.0 wavelength between centers (see Fig. 9) the trend in the measured field as the radius increases is closely predicted by the independent scattering hypothesis for ka ranging from zero to about 1.5. When the spacing is increased to 3.024 wavelengths (see Fig. 22) the independent scattering hypothesis gives a fiarly good prediction of the trend for ka as large 2.5. This simple assumption also predicts the over-all shape of the results in the cases where the probe is fixed, the radius is constant and the spacing allowed to vary from 1.0 to 8.0 wavelengths (see Figs 17 through 21).

In all the measurements referred to above there is practically no detailed agreement between the measurements and the results of the simple independent scattering hypothesis, even for ka as small as 0.0783 and a spacing of 3.024 wavelengths (see Fig. 22). The diffraction patterns in Fig. 15 and Fig. 16 show this same lack of detailed agreement. For example, the diffraction pattern (see Fig. 15) in which the cylinders are spaced 1.0 wavelength between centers with ka equal to 1.253 shows a maximum difference of approximately 50 percent between the measured and independent scattering results at the first minimum in pattern. Succeeding measured coupled and independent (scattering) minima and maxima are slightly shifted from one another and show amplitude differences of approximately 4 to 8 per cent. For the same spacing and ka equal 2.0 (see Fig. 16) there is a pronounced shift in pattern and greater differences in the amplitude of corresponding maxima and minima than in the case with ka equal to 1.253. All the data taken show in general, as might be expected, that the larger the radius and smaller the spacing the poorer becomes the detailed agreement between the predictions of the simple independent scattering hypothesis and the corresponding measurements. These measurements clearly indicate the need of a better theory to predict the detailed nature of the results, so attention will now be focussed on the specific results of the theory developed in Sections 4,5 and 6.

For small cylinders, only the zeroth mode or uniform-current mode is significant in calculating the scattered field. The range of radii and spacings over which this mode alone is sufficient is determined primarily by the radius,* since this parameter determines the number of modes required in the corresponding problem of diffraction by a single isolated cylinder. Thus with a fixed probe and constant spacing of 1.0 wavelength Fig. 9 shows that the uniform-current distribution gives excellent agreement with experiment for ka less than approximately 0.3. Incidentally it is interesting to note that the approximate shape of this entire experimental curve is reflected on a much exaggerated scale in the curve calculated from the use of only the zeroth mode. This mode is the one used by Wessel[5] in his analysis of the diffraction grating of small wires, and the validity of his theory for a large range of spacings (including smaller spacings than used here) has been established by the experiments of Esau, Ahrens and Kebbel.[19] The next step is to keep all the modes required for the same accuracy in the problem of diffraction by a single isolated cylinder. Due to the large amount of computing required, the effect of solving a finite number of equations for a fewer or greater number of modes has not been throughly investigated. However, in one case, that for ka equal to 1.253 with a spacing of 1.0 wavelength (see Fig. 15), a finite system was solved keeping at first three modes, and then four modes. Both cases lead to results in about equally close

- - - - - - -

*For cylinders and spacings very much less than a wavelength, the problem can be handled by the electrostatic approximation much as Lamb[22] treated the problem of a planar grating of small wires.

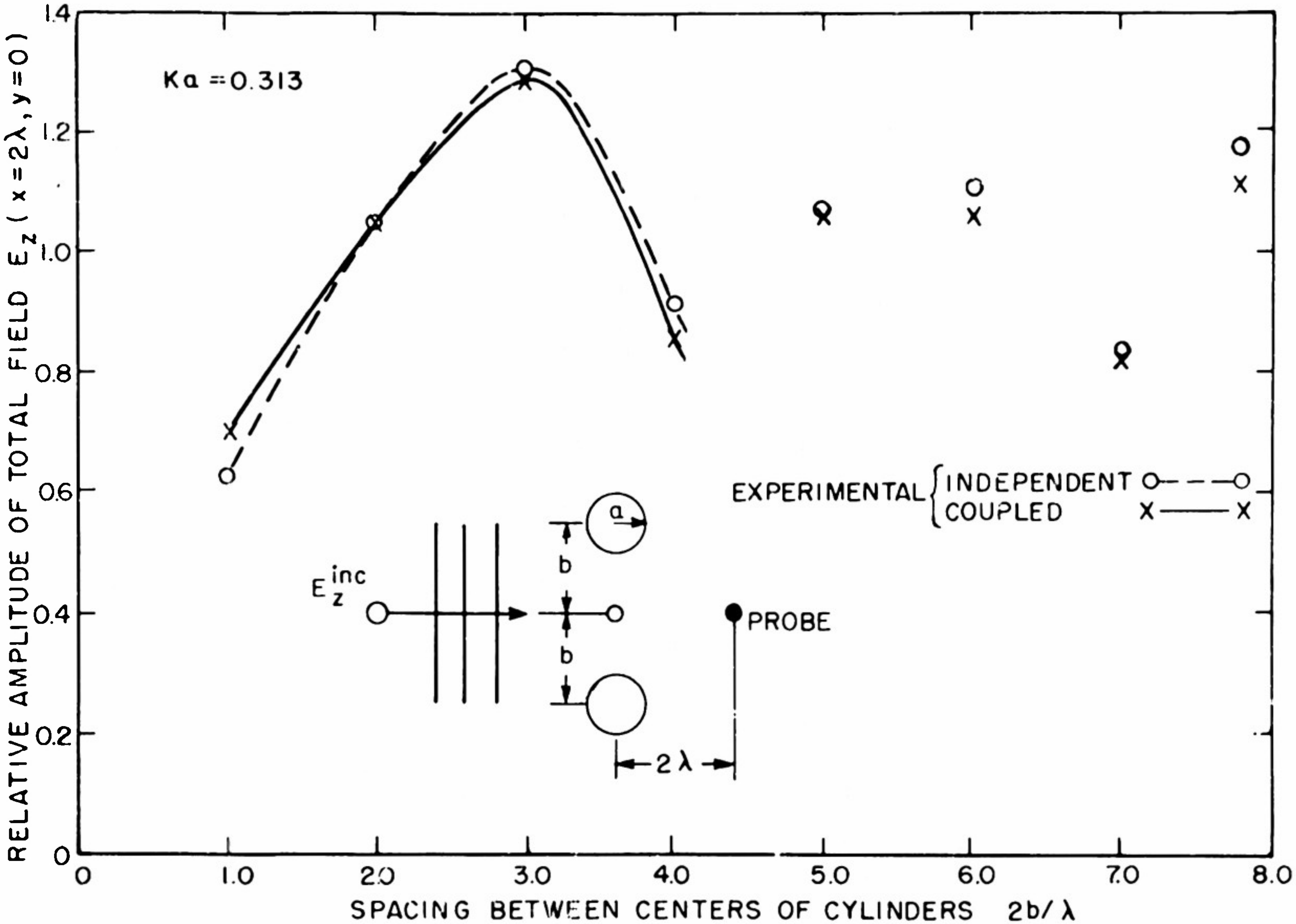

FIG. 17 EXPERIMENTALLY MEASURED INDEPENDENT AND COUPLED SCATTERING FROM TWO IDENTICAL CYLINDERS WITH Ka = 0.313 AS A FUNCTION OF SPACING. PROBE POSITION FIXED.

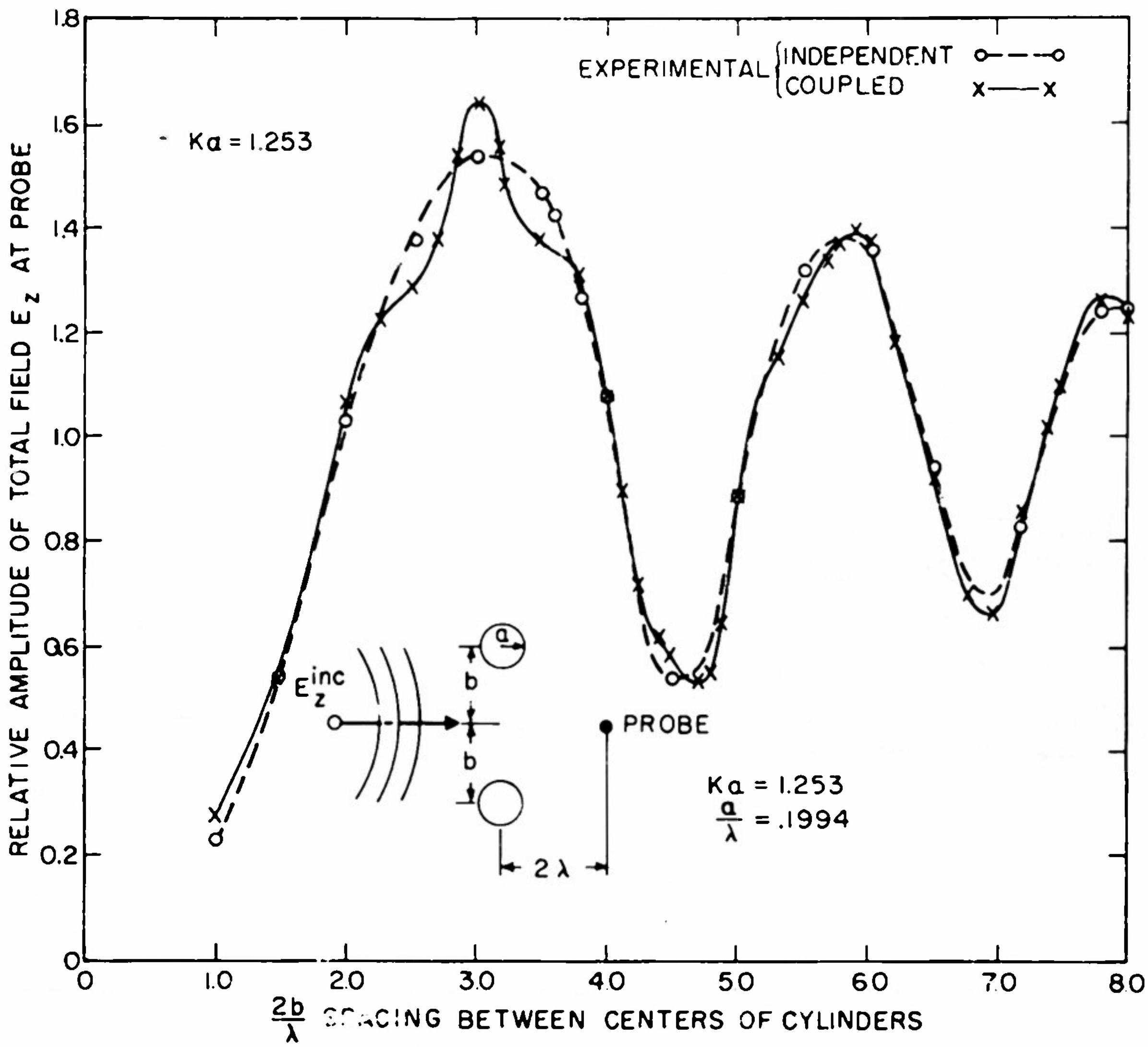

FIG. 18 EXPERIMENTALLY MEASURED INDEPENDENT AND COUPLED SCATTERING FROM TWO IDENTICAL CYLINDERS WITH Ka = 1.253 AS A FUNCTION OF SPACING. PROBE POSITION FIXED

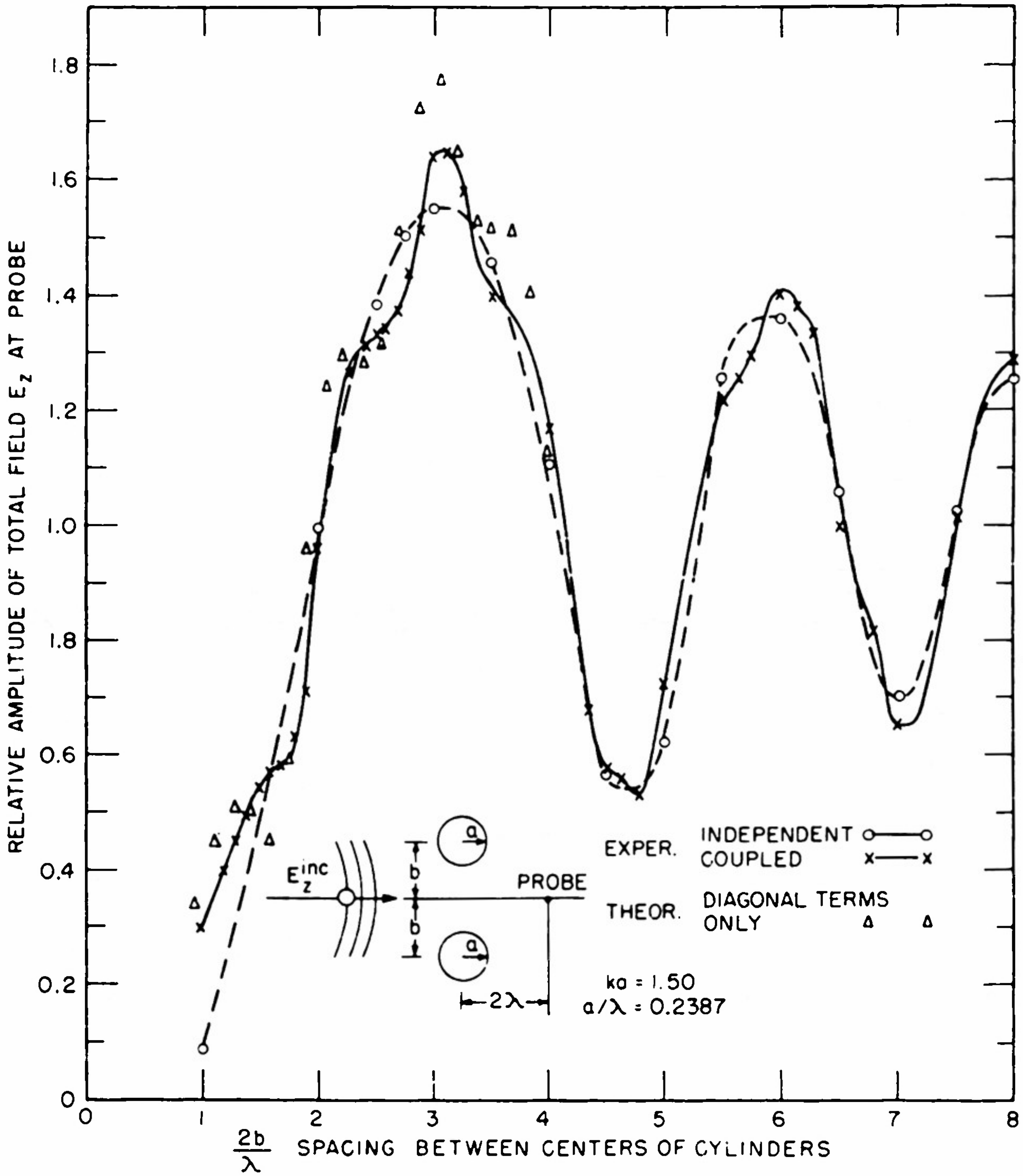

FIG. 19 EXPERIMENTAL MEASURED INDEPENDENT AND COUPLED SCATTERING FROM TWO IDENTICAL CYLINDERS WITH ka=1.50 AS A FUNCTION OF SPACING. PROBE POSITION FIXED.

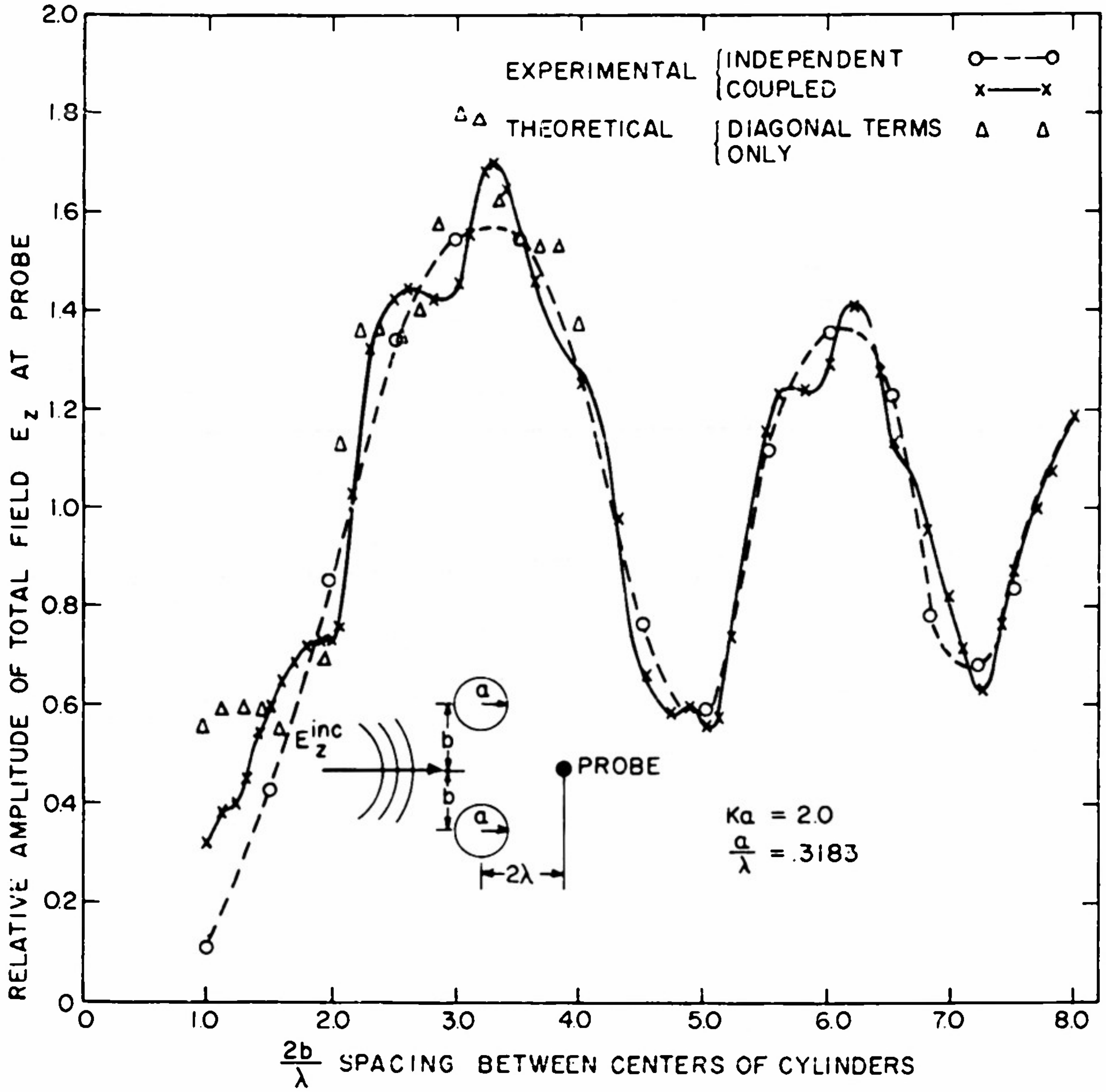

FIG. 20 EXPERIMENTALLY MEASURED INDEPENDENT AND COUPLED SCATTERING FROM TWO IDENTICAL CYLINDERS WITH Ka=2.0, AS A FUNCTION OF SPACING. PROBE POSITION FIXED.

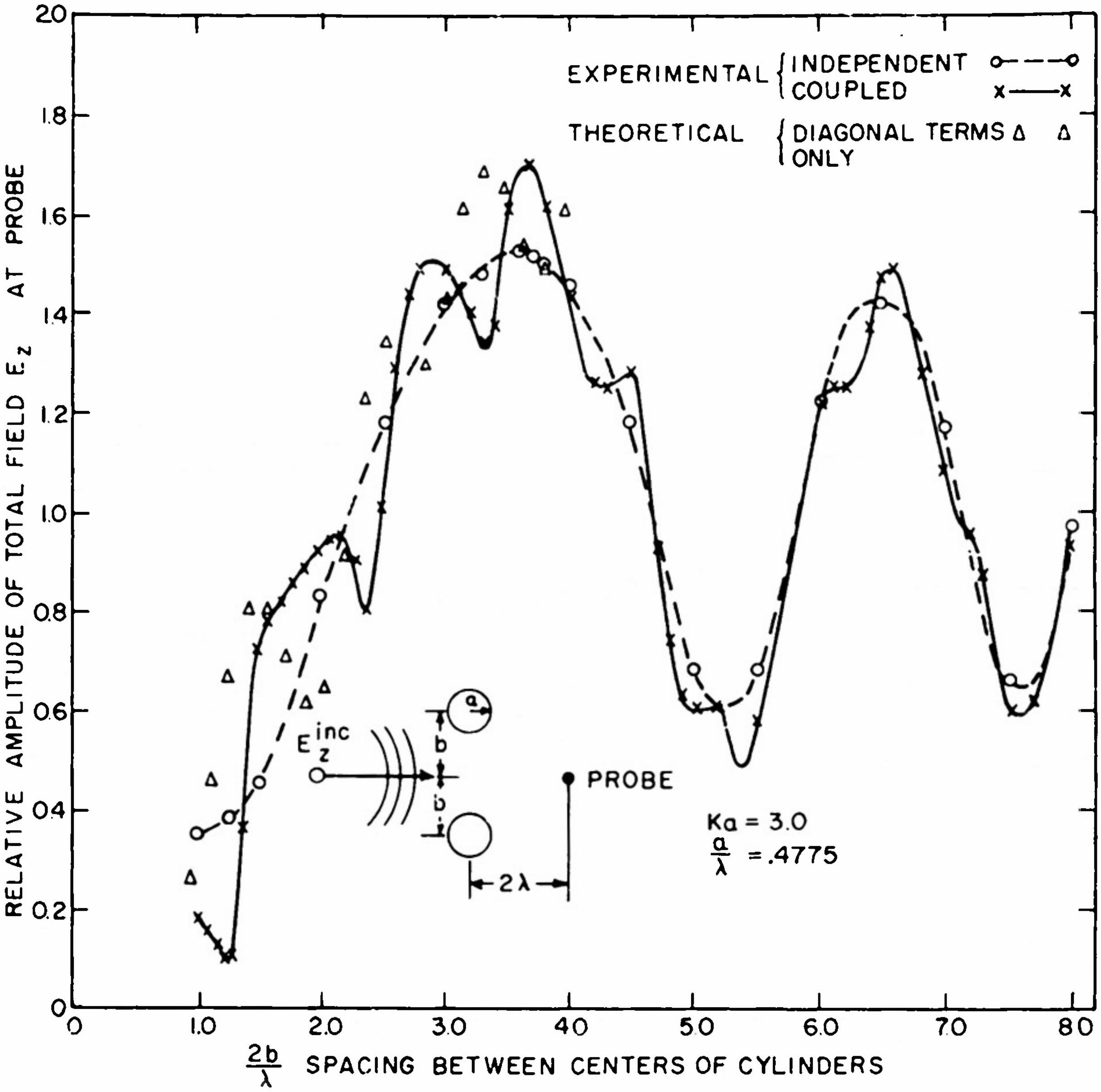

FIG. 21 EXPERIMENTALLY MEASURED INDEPENDENT AND COUPLED SCATTERING FROM TWO IDENTICAL CYLINDERS WITH Ka = 3.0 AS A FUNCTION OF SPACING. PROBE POSITION FIXED.

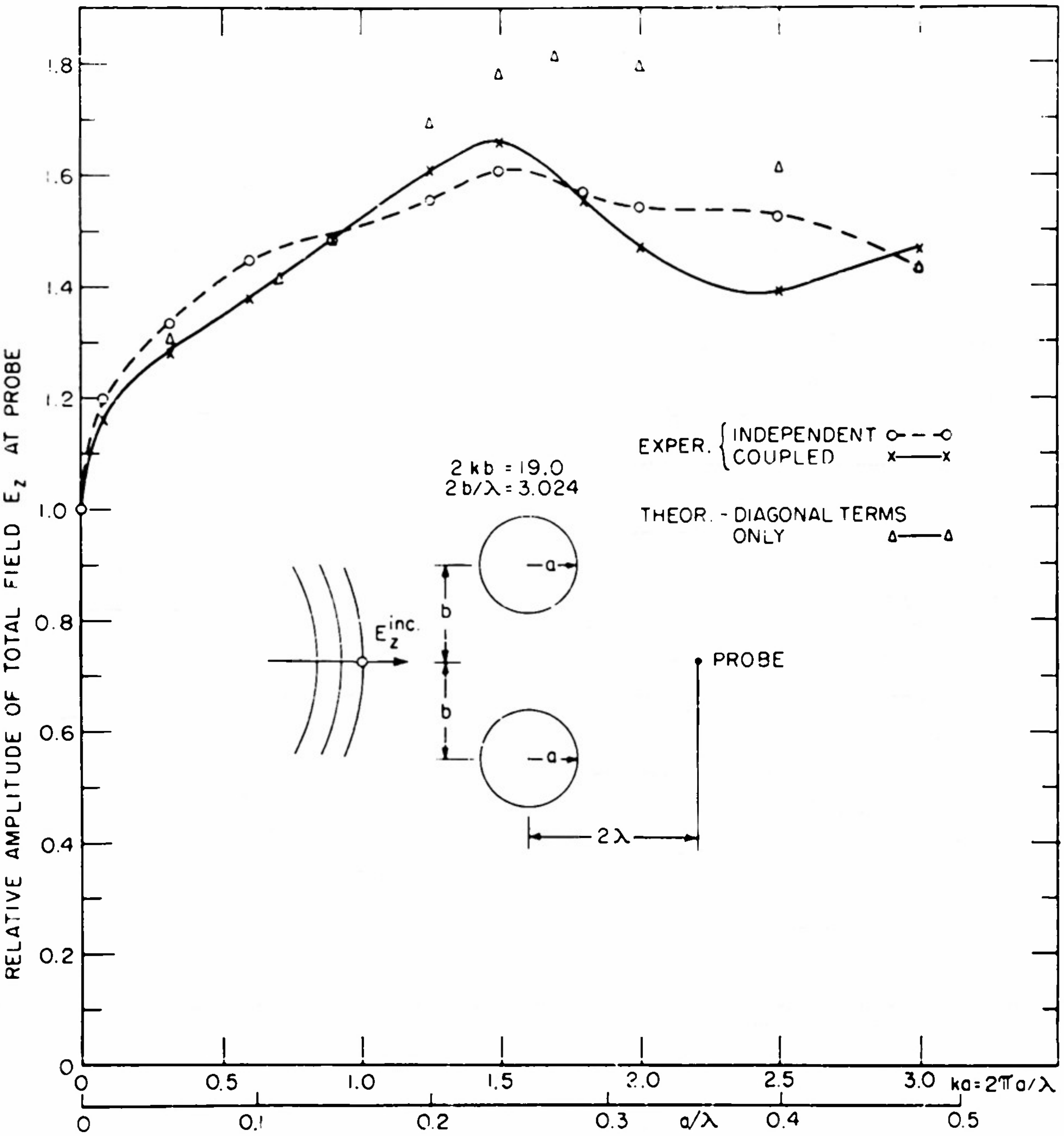

FIG. 22 AMPLITUDE OF FIELD SCATTERED BY TWO IDENTICAL CYLINDERS, FOR FIXED PROBE LOCATION AND SPACING $2b/\lambda = 1.0$ AS A FUNCTION OF RADIUS OF CYLINDERS

agreement with experiment. In all cases where the number of modes solved for was the same as required by the single-cylinder problem the detailed agreement between the theory and experiment is excellent.

The diffraction patterns (see Figs. 15 and 16) calculated (from the solutions to a finite number of linear equations) for a spacing of 1.0 wavelength and ka equal to 1.253 and 2.0 are in excellent agreement with the corresponding measured patterns. Likewise the points shown as triangles in Fig. 9 (showing the amplitude of the electric field at a fixed point as the radii of the cylinders are varied, with constant spacing) demonstrate the success of the theory developed in Section 4, where of course only a finite number of modes have been considered in solving the infinite matrix equation.

Without the use of large scale automatic calculating machinery it would be impracticable to compute the solutions to the system of equations (17) for any appreciable range of radii and spacings. Therefore the diagonal approximation introduced in Section 4 (pp. 29-34) has been used to compute the total field at a point equidistant from each cylinder and two wavelengths behind the line joining their centers, using formula (21) for $2b/\lambda$ equal to 1.0 and 3.024, and ka ranging from 0.0783 to 3.0 (Figs. 9 and 22); and for ka equal to 1.5, 2.0 and 3.0 and $2b/\lambda$ ranging from 1.0 to 4.0 (Figs. 19, 20 and 21). The corresponding experimental curves show significant coupling effects for spacing considerably greater than 4.0 wavelengths. However, convenient tables of the Neumann functions $Y_0(z)$ and $Y_1(z)$ are not available for z greater than 25.0 (corresponding to a maximum probe cylinder separation equivalent to a spacing of 4.0 wavelengths), and the most interesting coupling effects for all the cylinders measured occur for spacings less than four wavelengths.

From these results it is apparent that the diagonal approximation yields a satisfactory approximation to the shape of the experimental curves, even for the largest cylinders studied (ka equal to 3.0; a diameter of one wavelength corresponds to ka equal to π). For cylinders with ka less than approximately 1.5 the detailed point-by-point agreement between the theory and measurements is good and becomes better as the size of the cylinders decreases. In the curves taken with the radius constant there is a progressive shift in the peaks and valleys of the theoretical curves towards smaller spacings as the radius is increased, and for ka equal to 3.0 the first dip in the experimental curve is absent in the theory. These effects indicate the increasing need for considering interactions between modes of different order in the theory; that is, the mode coefficients must be obtained as the solutions to a 'block' from the matrix equation represented in Fig. 6.

The chief value of the 'diagonal' theory, then, is its usefulness in predicting the detailed shape of the experimental curves and showing that significant coupling effects do exist, and from the measurements it appears to give fairly good predictions of the location and magnitude of these effects for cylinders as large as a wavelength in diameter and spacings as little as a wavelength. The measurements also indicate that, with cylinders of diameter comparable to a wavelength, detailed point by point agreement between the diagonal theory and the measurements does not exist for spacings less than 4.0 wavelengths. What the spacing must be before a given degree of quantitative agreement is reached, has not been determined. However, it appears that most of the interesting coupling effects occur within the range of spacings for which computations were made.

<u>General Conclusions</u>.

The problem of the diffraction of a cylindrical wave by two identical conducting cylinders while not of great intrinsic physical interest in itself has served as a useful application of the very general theory developed in Section 3.—useful particularly in that it has allowed a comparison between the results of various approximations in the theory and measurements carried out on an actual physical arrangement of source and obstacles very closely approximating the conditions assumed in the theory. One approximation, the diagonal approximation, has proved very useful in predicting the shape of the experimentally measured curves for diameter and spacings comparable with a wavelength, where interesting and large coupling effects are found to exist. The diagonal approximation results in formulae not too difficult to compute which represents a great advantage, considering the labor required to solve a complete block from the matrix equation. The electric field amplitude as measured in the experiments is not of general physical interest as would be the scattering cross section or field-pattern. However, these quantities can be readily calculated once the mode coefficients are known, and the near-zone measurements served their purpose in conjunction with the theory.

The success of the diagonal approximation in the two-cylinder problem points encouragingly to the usefulness of the general method of analysis in handling the problem of the planar diffraction-grating (mentioned briefly in Section 3) of wires with diameter and spacing comparable to a wavelength. The same method of analysis and a similar diagonal approximation might prove fruitful in handling the problem of diffraction of a plane wave by a periodic array of spheres. Of course, the general method of analysis could be profitably extended to similar configurations lacking simplifying symmetry by the use of modern automatic computing machinery to solve the resulting systems of linear equations.

Due to the limitations of the experimental equipment, the theory has been formulated only for the case of the incident electric-vector parallel to the axes of the cylinders. However, the extension of the analysis to the other polarization should be straightforward.

Appendix A

EVALUATION OF THE INTEGRALS $_{tm}$ AND K_{tmns}

With reference to Fig. 1 of Section 3

$$r\Big|_{\text{on mth cylinder}} = \sqrt{r_m^2 + a_m^2 - 2r_m a_m \cos(\theta_m + \pi - \phi_m)} ,$$

and

$$r_m = \sqrt{r_o^2 + b_m^2 + 2r_o\, b_m \cos(\theta_o - \alpha_{om})} .$$

Using the addition theorem* for cylinder functions

$$H_o^{(1)}(Kr) = \sum_{\ell=-\infty}^{\infty} J_\ell(Ka_m)H_\ell^{(1)}(Kr_m)e^{i\ell(\theta_m+\pi-\phi_m)}$$

then

$$\gamma_{tm} = A\sum_{\ell}\int_0^{2\pi} J_\ell(Ka_m)H_\ell^{(1)}(Kr_m)e^{i\ell(\theta_m+\pi)-i\ell\phi_m-it\phi_m}d\phi_m$$

where interchanging the order of summation and integration is assumed to be valid. The orthogonality relations for the trigonometric functions enable γ_{tm} to be evaluated explicitly, hence

$$\gamma_{tm} = 2\pi AJ_t(Ka_m)H_t^{(1)}(Kr_m)e^{-it(\theta_m+\pi)}$$

It should be noted that for cylinders with centers above the line A-B in Fig. 1, θ_m is to be taken as positive and for those with centers below A-B it is negative.

The computation of K_{tmns} must proceed in two steps. The first case is that in which the indices m and n are equal, corresponding to r and r' lying on the surface of the same cylinder.

- - - - - - - -

*See Watson, "Theory of Bessel Functions," 2nd edition, MacMillan and Co., 1948, pp. 361.

With reference to Fig. A-1 for the case $n = m$,

$$|\vec{r} - \vec{r}'| = a_m\sqrt{1 - \cos(\phi_m-\phi_m')}$$

Using the above addition theorem for the cylinder functions gives us

$$K_{tmns} = \frac{1}{8\pi}\sum_{\ell}\int_0^{2\pi}\int_0^{2\pi} e^{is\phi_m'-it\phi_m} J_\ell(Ka_m)H_\ell^{(1)}(Ka_m)e^{i\ell(\phi_m-\phi_m')}d\phi_m d\phi_m'$$

$$= \frac{\pi i}{2} J_t(Ka_m)H_t^{(1)}(Ka_m)\delta_{st}$$

where

$$\delta_{st} = \begin{cases} 1 \text{ for } s=t \\ 0 \text{ for } s\neq t \end{cases}$$

Turning now to the evaluation of K_{tmns} when $n\neq m$. From Fig. B-1 it may be seen that

$$|\vec{r} - \vec{r}'| = \sqrt{s_{nm}^2 + a_n^2 - 2s_{nm}a_n \cos(\pi + \alpha_{nm} - \phi_n + \beta_{nm})}$$

Again applying the same addition theorem

$$K_{tmns} = \frac{1}{8\pi}\sum_{\ell}\int_0^{2\pi}\int_0^{2\pi} e^{is\phi_n-it\phi_m} J_\ell(ka_m)H_\ell^{(1)}(Ks_{nm})e^{i\ell(\pi+\alpha_{nm}-\phi_n-\beta_{n\beta})}d\phi_n d\phi_m$$

carrying out the ϕ_n integration we get

$$K_{tmns} = \frac{1}{4}\int_0^{2\pi} e^{-it\phi_m} J_s(Ka_n)H_s^{(1)}(Ks_{nm})e^{is(\pi+\alpha_{nm}+\beta_{nm})} d\phi_m \quad .$$

Both s_{nm} and β_{nm} are dependent on ϕ_m so that in order to perform the remaining integration the more general addition theorem*

$$H_s^{(1)}(Ks_{nm})e^{is\beta_{nm}} = \sum_{q=-\infty}^{\infty} J_q(Ka_m)H_{s+q}^{(1)}(K|\vec{b}_m-\vec{b}_n|)e^{iq(\alpha_{nm}-\phi_m)}$$

------

*Watson, "Bessel Functions," loc. cit.

must be used whence it may readily be shown that

$$K_{tmns} = \frac{\pi i}{2} J_t(Ka_m)J_s(Ka_n)H^{(1)}_{t-s}(K|\vec{b}_m-\vec{b}_n|)e^{-it\alpha_{nm} + is\alpha_{nm}}$$

Summarizing

$$\gamma_{tm} = 2\pi A J_t(Ka_m)H^{(1)}_t(Kr_m)e^{-it(\theta_m+\pi)}$$

$$K_{tmns} = \frac{\pi i}{2} J_t(Ka_m)\begin{cases} H^{(1)}_s(Ka_m)\ \delta_{st} , & n = m \\ J_s(Ka_n)H^{(1)}_{t-s}(K|\vec{b}_m-\vec{b}_n|)e^{-it\alpha_{nm}+is\alpha_{nm}}, & n \neq m \end{cases}$$

Appendix B

NUMERICAL SOLUTION OF THE MATRIX EQUATION K . a = 4iλ

Two methods of numerical solution have been used to solve a finite block from the infinite matrix equation for the spacing $2b/\lambda = 1.0$, and $Ka = 1.253$, 2.0 and 2.5.

The first method known as Crout's method* is especially well adapted to the solution of linear systems on a modern desk calculating machine and gives solutions to the same accuracy as the coefficients in the original system. The method will be described briefly so that an estimate can be made of the number of operations involved in the solution. The original matrix relation is written in the form

---

*See P. D. Crout, "A Short Method for Evaluating Determinants and Solving Systems of Linear Equations with real or Complex Coefficients, "Transactions of the American Institute of Electrical Engineers, 60, 1941.

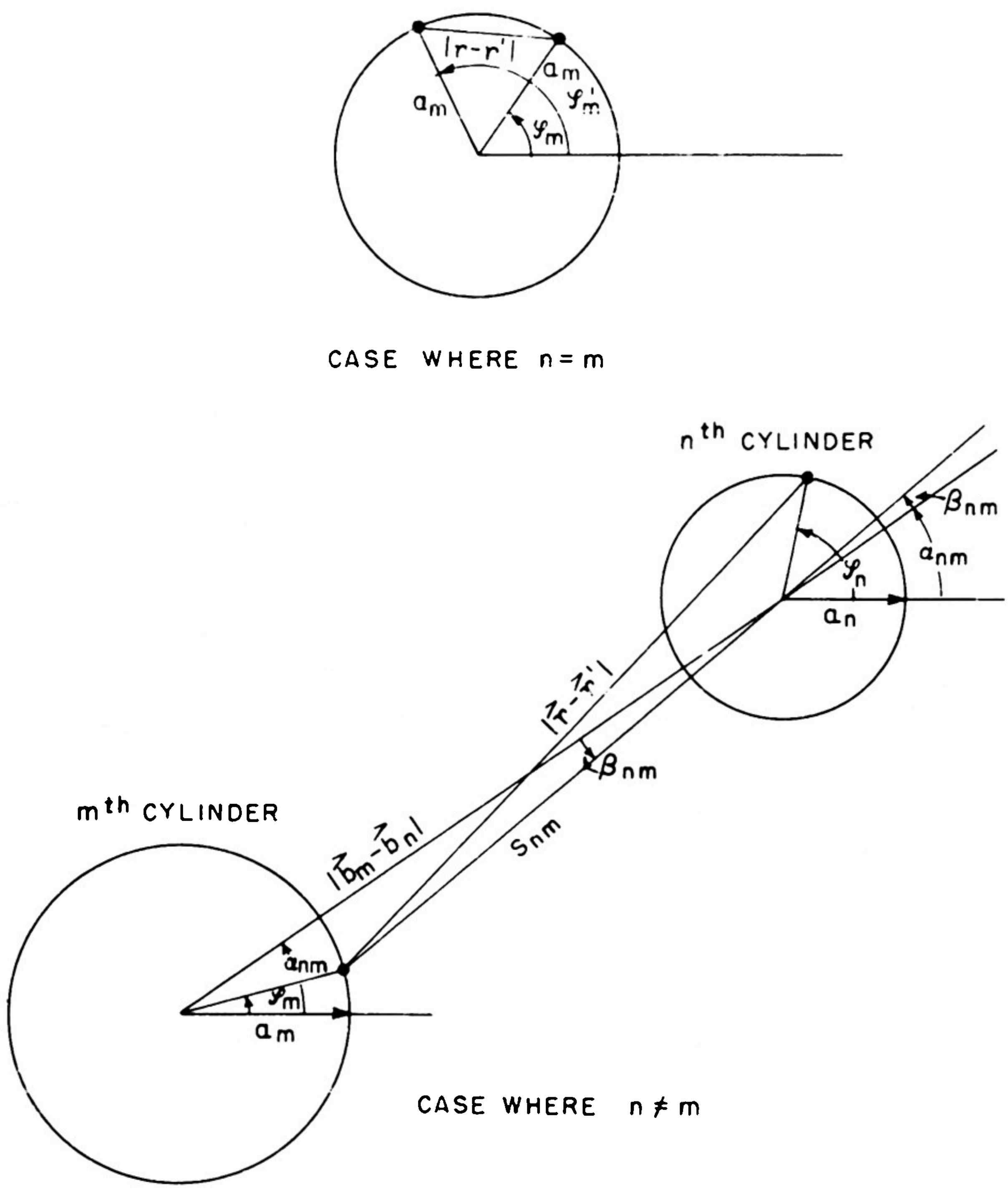

FIG. A-1 GEOMETRY FOR CALCULATION OF K_{tmns}

$$
\begin{array}{cccccc}
x_1 & x_2 & x_3 & \cdots & x_n & \\
\hline
a_{11} & a_{12} & a_{13} & \cdots & a_{1n} & = y_1 \\
a_{21} & a_{22} & \cdots & \cdots & a_{2n} & = y_2 \\
a_{31} & a_{32} & a_{33} & & a_{3n} & = y_3 \\
\vdots & & & & & \\
a_{n1} & a_{n2} & \cdots & \cdots & a_{nn} & = y_n
\end{array}
$$

From this an auxiliary matrix B

$$
\begin{array}{cccccc}
b_{11} & b_{12} & \cdots & \cdots & b_{1n} & b_{1,n+1} \\
b_{21} & b_{22} & \cdots & \cdots & b_{2n} & b_{2,n+1} \\
b_{31} & b_{32} & b_{33} & \cdots & b_{3n} & b_{3,n+1} \\
\vdots & & & & & \\
b_{n1} & b_{n2} & \cdots & \cdots & b_{nn} & b_{n,n+1}
\end{array}
$$

is formed and finally the solution

$$x_1 = \cdots\cdots\cdots \quad X_n = b_{n,n+1}$$

is obtained. The rules for determining the auxiliary and final matrix are as follows:

Auxiliary Matrix.

i) Elements in the first column equal corresponding elements in the original matrix.

ii) Elements in the first row equal corresponding elements in the first row of the original matrix divided by the diagonal element of the same row in the auxiliary matrix.

iii) All elements below the principal diagonal are formed by subtracting from the corresponding element in the original matrix the sum of products of the elements previously calculated in the same row and column of the auxiliary matrix. Thus $b_{32} = a_{32} - b_{31}b_{12}$ and $b_{33} = a_{33} - (b_{31}b_{13} + b_{32}b_{23})$.

iv) Elements to the right of the principal diagonal are formed as in iii) except that the result of this calculation is divided by the previously computed diagonal element in the same row of the auxiliary matrix. The numbered arrows indicate the order of operations in the forming of the auxiliary matrix.

Final Matrix. (order of calculation important)

i) $x_n = b_{n,n+1}$

$$x_{n-1} = b_{n-1,n+1} - b_{1n}x_n$$

$$x_{n-2} = b_{n-2,n+1} - (b_{1n}x_n + b_{1,n-1}x_{n-1})$$

$$\vdots$$

$$x_1 = b_{1,n+1} - \sum_{s,1}^{n+1} b_{1,s}x_s$$

The advantages of this method are that each step in the rules requires only one machine operation and that a check column may be readily carried along, as a check on each row of the auxiliary matrix. A study of the number of machine operations shows that in forming the auxiliary matrix the t^{th} row requires $t(n-t)$ operations, and the t^{th} column requires $(t-1)(n-t+1)$ operations where n is the number of unknowns. In addition there are $n^2 - n$ original entries in the machine. Hence the total number of machine operations in setting up the auxiliary matrix is

$$n^2 - n + \sum_{t=1}^{n} \left\{ t(n-t) + (t-1)(n-t+1) \right\}$$

$$= \frac{n}{3}(n^2 + 3n - 5)$$

In addition there are $\frac{n(n-1)}{2}$ operations in the final matrix. Hence there a total of $\frac{n}{3}(n^2+9n-13)$ operations in the solution. Thus for ka = 2.0, the mode coefficients $a_{1,5} \ldots a_{10} \ldots a_{1-5}$ must be calculated. This means that there are 11 complex unknowns or equivalently 22 real unknowns requiring 4906 machine operations if no errors are made. Carrying a check column which is a necessity when there are so many variables requires another $n(n+2)$ operations for a total of 5634 operations.

The other method of solution is the Gauss-Seidel iteration procedure* based on a least-squares approximation to the true solution. The process can be shown to coverge in general. Consider the linear system

$$\begin{array}{lllll}
a_{11}x_1 & + & a_{12}x_2 + \cdots\cdots & a_{1n}x_n & = C_1 \\
a_{21}x_1 & + & a_{22}x_2 + \cdots\cdots & a_{2n}x_n & = C_2 \\
\vdots & & & & \\
a_{n1}x_1 & + & \cdots\cdots\cdots\cdots & a_{nn}x_n & = C_n
\end{array}$$

---

*See Whittaker and Robinson, Calculus of Observations, Blackie and Sons, London, 4th edition, p. 255.

As a first guess at the solution try

$$x_1^{(0)} = \frac{C_1}{a_{11}}, \quad x_2^{(0)} = \frac{C_2}{a_{22}}, \quad \ldots\ldots\ldots \quad x_n^{(0)} = \frac{C_n}{a_{nn}}$$

then form

$$N_1 = a_{11}x_1^{(0)} + a_{12}x_2^{(0)} + \ldots\ldots\ldots a_{1n}x_n^{(0)} - C_1$$

and

$$\Delta x_1^{(0)} = -\frac{N_1}{a_{11}}, \qquad x_1^{(1)} = x_1^{(0)} + \Delta x_0^{(0)}$$

Similarly

$$N_2 = a_{21}x_1^{(1)} + a_{22}x_2^{(0)} + \ldots a_{2n}x_n^{(0)} - C_2$$

$$\Delta x_2^{(0)} = -\frac{N_2}{a_{22}}, \quad \text{and } x_2^{(1)} = x_2^{(0)} + \Delta x_2^{(0)},$$

and so on, till all values $x_1^{(1)}, x_2^{(1)}, x_3^{(1)} \ldots x_n^{(1)}$ have been calculated. Then repeat this process over to obtain $x_1^{(2)}, x_2^{(2)} \ldots$ etc. As in every true iteration process, errors made in the calculations are automatically compensated for.

The computation of $x_1^{(0)}, x_2^{(0)} \ldots x_n^{(0)}$ requires n divisions and the succeeding processes to obtain $x_1^{(1)}, x_2^{(1)} \ldots$, etc. require n+2 operations for a total of n | + n(+2) zeroth-order solution operations in the first iteration. If N iterations are carried through, the total number of operations is

$$n + Nn(n+2) \quad .$$

Thus for Ka = 2.0 it was found that 4 iterations were necessary to reduce the changes in the unknowns with further iteration to less than 1 percent. Thus the total number of machine operations would be 2134.

It is apparent then that at least 1 percent accuracy in the final solutions may be obtained by the iteration procedure with less than half the number of operations required by the exact method of solution described previously. So the iterative method

SOLUTIONS TO $Ka = 4i\lambda$ FOR $Ka = 1.253$, $\frac{2b}{\lambda} = 1.0$

ITERATED SOLUTION (SYSTEM SOLVED FOR $a_{14} \ldots a_{10} \ldots a_{1-4}$

NUMBER OF ITERATIONS	a_{14}	a_{13}	a_{12}	a_{11}	a_{10}	a_{1-1}	a_{1-2}	a_{1-3}	a_{1-4}
1	0.01460 0.03135i	0.1668 -0.3333i	-0.9767 0.8630i	-1.035 1.644i	0.9982 -0.7665i	0.009900 0.8860i	-0.8541 0.6001i	0.4088 -0.1102i	0.04156 0.049751i
2	0.02065 0.03216i	0.1876 -0.3340i	-0.9148 -0.8500i	-0.9708 1.507i	1.138_5 -0.4973i	-0.06540 0.8389i	-0.8126 -0.6540	0.3884 -0.09886i	0.04621 0.008449i
3	0.02000 0.03153i	0.1837 -0.3337i	-0.9263 -0.8427i	-0.9594 1.528	1.139_4 -0.5247i	-0.05568 0.8268i	-0.8184 -0.6484i	0.3910 -0.09944i	0.04532 0.007887i
4	0.02008 0.03137i	0.1870 -0.3347i	-0.9272 -0.8448i	-0.9652 1.532	1.145 -0.5219i	-0.05300 0.8269i	-0.8197 -0.6499i	0.3912 -0.09875i	0.04547 0.007696i
5	—	—	—	—	1.1449 -0.5201i	—	—	—	—

EXACT SOLUTION (SYSTEM SOLVED FOR $a_{12} \ldots a_{10} \ldots a_{1-2}$

	a_{14}	a_{13}	a_{12}	a_{11}	a_{10}	a_{1-1}	a_{1-2}	a_{1-3}	a_{1-4}
	—	—	-0.8871 -0.8720i	-0.7574 1.377i	1.307 -0.4319i	-0.05425 0.9633i	-0.8286 -0.6469i	—	—

EXACT SOLUTION (SYSTEM SOLVED FOR $a_{11} \ldots a_{10} \ldots a_{1,-1}$

	a_{14}	a_{13}	a_{12}	a_{11}	a_{10}	a_{1-1}	a_{1-2}	a_{1-3}	a_{1-4}
	—	—	—	-1.024 1.338i	1.151 -0.6622i	-0.05974 1.018i	—	—	—

FIGURE B-1

alone has been used in the solution for Ka = 2.0 and 2.5 and both the iterative and Crout's method used for the solutions for Ka = 1.253.

The following tables shows the value of the unknowns a_{14}, a_{13} . . . . . . $a_{1,0}$ . . . . . a_{1-3}, $a_{1,-4}$ for Ka = 1.253 and $2b/\lambda = 1$ after 1, 2, 3 and 4 iterations. In addition the solutions by Crout's method for a_{12} . . . . . a_{10} . . . . . a_{1-2} are given for comparison. The values of the unknowns have been rounded off to four figures in the table, although in practice as many figures were kept as the desk calculator would hold. A factor 41 x 0.0529918 has been removed from the right-hand side of the equations before solution.

Acknowledgments

The writer is indebted to Misses M. Tynan and E. Miller and to Mrs. M. Amith for assistance with the computations. Dr. J. E. Storer contributed helpfully in discussions on the theory, and Mr. E. Roffey modified the parallel-plate apparatus to allow measurements to be made of scattering by two cylinders.

References (continued)

14. J. W. Miles, Quart. Appl. Math. 7, 45 (1949).

15. C. Shaefer and F. Reiche, Ann. der Physik 35, 817 (1911).

16. W. Seitz, Ann. der Physik 16, 746 (1905), and Ann. der Physik 19, 554 (1908).

17. F. Zaviska, Ann. der Physik 40, 1023 (1913).

18. C. L. Shaefer and F. Grossman, "Beugung der ebener Wellen an einem Zylinder usw," Ann. der Physik 31, 455 (1910).

19. A. Esau, E. Ahrens and W. Kebbel, "Uber die Durchlässigkeit von Drahtgittern usw," Hochfrequenz und Electroakustik, 53, 113-115 (1939).

20. W. Franz, Zeitschrift fur Angewandte Physik 1, 9, 416-423 (1949).

21. V. Twersky, Jour. Appl. Phys. 23, 1099 (1952).

22. "Scattering and Radiation from Circular Cylinders and Spheres," Tables Of Amplitudes and Phase Angles, Prepared by A. N. Lowan, P. M. Morse, H. Freshbach and M. Lax, Massachusetts Institute of Technology, Contract OEMse-1046, February, 1945.

Bibliography of Useful General References and Tables

G. N. Watson, A Treatise on the Theory of Bessel Functions, 2nd ed., Cambridge University Press, 1948.

P. M. Morse and H. Feshbach, "Methods of Theoretical Physics," Mimeographed notes from the Department of Physics, Massachusetts Institute of Technology, Cambridge, Massachusetts.

Vector Diffraction Theory

J. A. Stratton, Electromagnetic Theory, McGraw-Hill, New York, 1st ed., 1941. See especially the section on diffraction of a plane wave by a sphere, p. 563.

H. Levine and J. Schwinger, "On the Theory of Electromagnetic Wave Diffraction by an Aperture in an Infinite Plane Conducting Screen," Communications on Pure and Applied Mathematics, New York University, Vol. 3, No. 4 (1950). This paper gives numerous references to existing work on the theory of vector electromagnetic scattering.

<u>Tables</u>

"Tables of Bessel Functions of the First Kind of Orders 0,1,2,3; 4,5,6;7,8,9." Arg. 0 x 25, steps of 0.001, Arg. 25 x 100 steps of 0.01. Harvard university Press.

"British Association Mathematical Tables VI, Bessel Function Part I." These are the most extensive existing tables of $Y_0(x)$ and $Y_1(x)$ for 0 x 25 dt steps of 0.01 and auxiliary functions to calculate these functions for 25 x 50 with second differences in steps of 0.1, x 50 150, steps of 1, 150 x 1150 steps of 50, 1000 x 6000, steps of 100. Cambridge University Press, 1950.

Tafeln für die Differenzenrechnung sowie für die Hyperbel, Besselschen, Elliptischen und Anderen Funktionen von Keuchi Hayashi, gives tables of $Y_n(x)$ for n, 0 to 30 in steps of 1, 16 x 25 in steps of 1.0. Julius Springer, Berlin, 1933.

Seven-Place Values of Trigonometric Functions Compiled by Dr. J. Peters, in steps of 0.001 degree, Van Nostrand, New York, 1942.

Additional Reports Issued by Cruft Laboratory

(under Contract N5ori-76)

in the Field of Electromagnetic Radiation

No.

2 D. D. King, "Measured Impedance of Cylindrical Dipoles," 1946. J. Appl. Phys., Oct. 1946.

6 D. D. King, "Impedance Measurements on Transmission Lines," 1946. Proc. I.R.E., May 1947.

8 B. C. Dunn, Jr. and R. W. P. King, "Currents Excited on a Conducting Plane...," 1947. Proc. I.R.E., Feb. 1948.

11 D. D. King et al, "Bolometer Amplifier for Minimum Signals," 1947. Electronics, Feb. 1948.

12 C. T. Tai, "Theory of Coupled Antennas," 1947. Part I Proc. I.R.E., April 1948; Part II, ibid, Nov. 1948.

16 Tung Chang, "Impedance Measurements of Antennas Involving Loop and Linear Elements," 1947.

18 C. T. Tai, "Propagation of Electromagnetic Waves from a Dissipative Medium to a Perfect Dielectric," 1947.

20 R. W. P. King, "Graphical Representation of the Characteristics of Cylindrical Antennas," 1947.

22 C. H. Papas and R. W. P. King, "Radiation Resistance of End-Fire Collinear Arrays," 1947. Proc. I.R.E., June 1948.

23 R. W. P. King, "Field of Dipole with Tuned Parasite at Constant Power," 1947. Proc. I.R.E., July 1948.

25 J. V. Granger, "Low-Frequency Aircraft Antennas," 1947.

27 C. H. Papas and R. W. P. King, "Surface Currents on a Conducting Plane...," 1948. J. Appl. Phys., Sept. 1948.

28 C. T. Tai, "Reflection and Refraction of a Plane Electromagnetic Wave...," 1948.

32 C. H. Papas and R. King, "Currents on the Surface of an Infinite Cylinder," 1948. Quart. Appl. Math., Jan. 1949.

35 P. Conley, "Impedance Measurements with Open-Wire Lines," 1948. J. Appl. Phys., Nov. 1949.

39 S. B. Cohn, "Theoretical and Experimental Study of a Waveguide Filter Structure," 1948.

40 C. T. Tai, " Reflection of Plane Electromagnetic Waves from Perfectly Conducting Grounded Half-Cylinder," 1948.

41 R. W. P. King, "Theory of Antennas Driven from a Two-Wire Line," 1948. J. Appl. Phys., Sept. 1949.

42 J. V. Granger, "Note on Broad-Band Impedance Characteristics of Folded Dipoles," 1948.

43 D. G. Wilson and R. King, "Measurement of Antenna Impedance Using Receiving Antenna," 1948.

44 E. Hallen, "Properties of Long Antennas," 1948. J. Appl. Phys., Dec. 1948.

46 E. Hallen, " Admittance Diagrams for Antennas...," 1948.

47 C. T. Tai, "On the Theory of Biconical Antennas," 1948. J. Appl. Phys., Dec. 1948.

48. K. Tomiyasu, "Problems of Measurement on Two-Wire Lines with Application to Antenna Impedance," 1948. Condensed version, J. Appl. Phys., Oct. 1949.

49 E. Hallen, "Traveling Waves and Unsymmetrically Fed Antennas, 1948.

50 D. D. King, "Measurement and Interpretation of Antenna Scattering," 1948.

52 C. H. Papas and R. King, "Input Impedance of Wide-Angle Conical Antennas," 1948. Proc. I.R.E., Nov. 1949.

53 D. K. Reynolds, "Surface-Current and Charge Measurements on Flat Metal Sheets," 1948.

55 C. T. Tai, "Study of the EMF Method," 1948. J. Appl. Phys., July 1949.

56 T. W. Winternitz, "The Cylindrical Antenna Center-Driven by a Two-wire Open Transmission Line," 1948. Quart. Appl. Math., 1949.

58 C. H. Papas, "On the Infinitely Long Cylindrical Antenna," 1948. J. Appl. Phys., May 1949.

61 C. H. Papas, "Radiation from a Transverse Slot in an Infinite Cylinder," 1948. J. Math. and Phys., Jan. 1950.

63 J. V. Granger and N. G. Altman, "Full-Scale Aircraft Antenna Measurements," 1949.

66 T. Morita, "Measurement of Current and Charge Distributions on Cylindrical Antennas," 1949. Proc. I.R.E., Aug. 1950.

67 T. Morita and C. E. Faflick, "Measurement of Current Distributions along Coupled Antennas...," 1949.

69 J. E. Storer and R. King, "Radiation Resistance of a Two-Wire Line," 1949.

70 J. V. Granger, "Shunt-Excited Flat-Plate Antennas...," 1949. Proc. I.R.E., March 1950.

71, 72, 73 B. C. Dunn, Jr., "Microwave Field Measurements," I (with R. King), II and III, 1949.

74 R. King and K. Tomiyasu, "Terminal Impedance and Generalized Two-Wire Line Theory," 1949. Proc. I.R.E., Oct. 1949.

75 C. T. Tai, "Application of a Variational Principle to the Study of Biconical Antennas," 1949.

76 C. H. Papas, "Radiation from a Circular Diffraction Antenna," 1949.

77 C. T. Tai, "On Radiation and Radiating Systems in the Presence of a Dissipative Medium," 1949.

78 J. V. Granger and T. Morita, "Current Distribution on Aircraft," 1949.

81 K. Tomiyasu, "Loading and Coupling Effects of Standing-Wave Detectors," 1949. Proc. I.R.E., Dec. 1949.

83 C. H. Papas, "Diffraction by a Cylindrical Obstacle," 1949. J. Appl. Phys., April 1950.

84 R. King, "Theory of N Coupled Parallel Antennas," 1949. J. Appl. Phys., Feb. 1950.

86 K. Tomiyasu, "Unbalanced Terminations on a Shielded-Pair Line," 1949.

91 R. King, "Theory of Collinear Antennas," 1949.

92 C. H. Papas and R. King, "Radiation from Wide-Angle Conical Antennas...," 1949. Proc. I.R.E., Nov. 1949.

93 R. King, "Asymmetrically Driven Antennas and the Sleeve Dipole," 1949.

94 T. Morita, E. O. Hartig, and R. King, "Measurement of Antenna Impedance...," (Supplement to T. R. 43), 1949.

95 C. P. Hsu, "Theory of Helical Waveguides and Helical Radiators," 1950.

96 R. King, "Theory of V-Antennas," 1950.

98 D. J. Angelakos, "Current and Charge Distributions on Antennas and Open-Wire Lines," 1950.

100 H. Levine and C. H. Papas, "Theory of the Circular Diffraction Antenna," 1950.

101 J. E. Storer, "Variational Solution to the Problem of the Symmetrical Cylindrical Antenna," 1950.

105 R. D. Kodis, "An Experimental Investigation of Microwave Diffraction," 1950.

107 E. O. Hartig, "Circular Apertures and their Effects on Half-Dipole Impedances," 1950.

108 E. O. Hartig, "A Study of Coaxial-Line Discontinuities Using a Variational Method," 1950.

101 J. E. Storer, "Variational Solution to the Problem of the Symmetrical Cylindrical Antenna," 1950.

104 G. Wheeler, "Coupled Slot Antennas," October 25, 1950.

105 R. D. Kodis, "An Experimental Investigation of Microwave Diffraction," 1950.

107 E. O. Hartig, "Circular Apertures and Their Effects on Half-Dipole Impedances," 1950.

109 E. O. Hartig, "An Experimental and Theoretical Discussion of the Circular Diffraction Antenna," 1950.

118 R. King, "Self- and Mutual Impedances of Parallel Identical Antennas," 1950.

119 J. E. Storer, "The Impedance of an Antenna over a Large Circular Screen," 1950. J. Appl. Phys., August 1951.

121 R. King, "Theory of Collinear Antennas, II," 1950. J. Appl. Phys., December 1950.

122 J. Taylor and T. Morita, "Antenna Pattern-Measuring Range," 1951.

126 J. E. Storer, "The Radiation Pattern of an Antenna over a Circular Ground Screen," 1951.

128 J. Taylor, "The Sleeve Antenna," 1951.

129 T. E. Roberts, Jr., "Currents Induced on an Infinitely Long Wire by a Slice Generator," 1951.

130 R. King, "A Dipole with a Tuned Parasite: Theory and Experiment," 1951. J.I.E.E., January 1952.

132 R. King, "An Improved Theory of the Receiving Antenna," June 1951.

134 T. E. Roberts, Jr., "Properties of a Single-Wire Line," 1951.

138 C. Huang and R. D. Kodis, "Diffraction by Spheres and Edges at 1.25 Centimeters," 1951.

139 T. E. Roberts, Jr., "An Experimental Investigation of the Single-Wire Transmission Lien," 1952.

141 R. King, "Theory of Electrically Short Transmitting and Receiving Antennas," 1952.

146 C. Moritz, "The Coupled Receiving Antenna, I.," 1952.

147 C. Moritz, "The Coupled Receiving Antenna, II.," 1952.

148 C. H. Papas and D. B. Brick, "Radiation of the Boss Antenna," 1952.

149 J. Sevick and J. E. Storer, "A General Theory of Plane-Wave Scattering from Finite Conducting Obstacles with Application to the Two-Antenna Problem," 1952.

150 J. Sevick "Experimental and Theoretical Results on the Back-Scattering Cross Section of Coupled Antennas," 1952.

151 J. Sevick, "An Experimental Method of Measuring Back-Scattering Cross Sections of Coupled Antennas," 1952.

152 J. E. Storer "Wave Propagation in a Two-Dimensional Periodic Medium," 1952.

153 R. V. Row, "Microwave Diffraction Measurements in a Parallel-Plate Region," 1952.

154 R. King, "An Alternative Method of Solving Hallén's Integral Equation and its Application to Antennas near Resonance," 1952.

159 L. S. Sheingold, "The Susceptance of a Circular Obstacle to an Incident Dominant Circular-Electric Wave," 1952.

160 J. E. Storer, L. S. Sheingold, and S. Stein, "A Simple Graphical Analysis of Waveguide Junctions," 1952.

162 T. Morita and L. S. Sheingold, "A Coaxial Magic-T," 1952.

163 "On the Diffraction of Electromagnetic Waves by Annular, Elliptical and Rectangular Apertures," C. Huang, February 1953.

166 "Circumferential Gap in a Circular Waveguide Excited by a Dominant Circular-Electric Wave," L. S. Sheingold and J. E. Storer, March 1953.

170 "Electromagnetic Scattering from Two Parallel Conducting Circular Cylinders." R. V. Row, May 1953.

173 "A Tabulation of Fresnel Integrals," R. Turner and A. Downey, May 1953.